



HAL
open science

A Century of Nonlinearity in the Geosciences

Michael Ghil

► **To cite this version:**

Michael Ghil. A Century of Nonlinearity in the Geosciences. Earth and Space Science, 2019, 6, pp.1007-1042. 10.1029/2019EA000599 . insu-03727019

HAL Id: insu-03727019

<https://insu.hal.science/insu-03727019>

Submitted on 28 Jul 2022

HAL is a multi-disciplinary open access archive for the deposit and dissemination of scientific research documents, whether they are published or not. The documents may come from teaching and research institutions in France or abroad, or from public or private research centers.

L'archive ouverte pluridisciplinaire **HAL**, est destinée au dépôt et à la diffusion de documents scientifiques de niveau recherche, publiés ou non, émanant des établissements d'enseignement et de recherche français ou étrangers, des laboratoires publics ou privés.



Distributed under a Creative Commons Attribution - NonCommercial - ShareAlike 4.0 International License

Earth and Space Science



REVIEW ARTICLE

10.1029/2019EA000599

Special Section:

Nonlinear Systems in Geophysics:
Past Accomplishments and Future
Challenges

Key Points:

- Nonlinear concepts and methods have greatly expanded the range of problems we can address
- There is still only a small but increasing number of nonlinear methodologies
- Prediction is a great test of our mathematical and physical understanding

Correspondence to:

M. Ghil,
ghil@atmos.ucla.edu

Citation:

Ghil, M. (2019). A century of nonlinearity in the geosciences. *Earth and Space Science*, 6, 1007–1042. <https://doi.org/10.1029/2019EA000599>

Received 18 FEB 2019

Accepted 5 MAY 2019

Accepted article online 17 MAY 2019

Published online 12 JUL 2019

©2019. The Authors.

This is an open access article under the terms of the Creative Commons Attribution-NonCommercial-NoDerivs License, which permits use and distribution in any medium, provided the original work is properly cited, the use is non-commercial and no modifications or adaptations are made.

A Century of Nonlinearity in the Geosciences

Michael Ghil^{1,2} 

¹Department of Geosciences and Laboratoire de Météorologie Dynamique (CNRS and IPSL), Ecole Normale Supérieure, PSL Research University, Paris, France, ²Department of Atmospheric and Oceanic Sciences, University of California, Los Angeles, CA, USA

Abstract This paper provides a thumbnail sketch of the evolution of nonlinear ideas in the mathematics and physics of the geosciences, broadly construed, over the last hundred or so years. It emphasizes the mathematical concepts and methods and outlines simple examples of how they were, are, and maybe will be applied to the solid Earth—that is, the crust, mantle, and core—and its fluid envelopes—that is, the atmosphere and oceans.

Plain Language Summary Nonlinearity has become a buzzword, along with chaos, complexity, fractals, networks, tipping points, turbulence, and other concepts associated with modern science. We outline here what it all means and how it has affected the progress of the geosciences over the past century, mostly over the last six decades or so.

1. Introduction and Motivation

As we are celebrating 100 years since the founding of the American Geophysical Union, it is timely to consider the way that nonlinear concepts and methods have modified the way that we are practicing the geosciences today and may practice them over the next century.

While nonlinear approaches have rapidly expanded over the last half century, it is clear that their roots go back much further. One of the oldest nonlinear problems in the geosciences is certainly drawing a right angle on the face of the Earth, for example, between a meridian and a parallel: this problem is equivalent to solving the Diophantine equation $a^2 + b^2 = c^2$. It is conjectured that the ancient Egyptians applied this equivalence, commonly called Pythagoras's theorem, to build their pharaonic projects, from the basis up; specifically, that they used the simplest solution—namely, $(a, b, c) = (3, 4, 5)$ —by tying 12 = 3 + 4 + 5 equidistant knots into a rope and used it in order to build the great pyramids of Giza, and many other temples, palaces, and tombs (e.g., Cooke, 2011).

But that is, of course, not what we all have in mind when discussing nonlinearity in the sciences in general and in the geosciences in particular. Linear approaches dominated the physical sciences in the nineteenth century; the explosion of a variety of methodologies that deviate from them is well illustrated by the saying, often attributed to Stanislaw Ulam (Gleick, 1987), that linear dynamics is akin to elephant zoology, or words to that effect. What we mean by tracing back the rapid rise of nonlinear dynamics, nonlinear sciences, or what not to some time after World War II, is the following fact: according to the well-known story of the lamppost, and of attempts to find the forlorn keys in its circle of light, a superb development of methods for solving linear algebraic and differential equations in the nineteenth century led to great emphasis on solving problems formulated in terms of such equations in the first half of the twentieth century.

Basically, linear problems are easily separable, and hence solvable, due to the superposition principle, projection onto orthonormal bases, and so on. Thus, many such problems were solved over the last 200 years, most often analytically, that is, with pencil and paper or with very rudimentary computational devices. And these methods are still of great use to us, in deriving and determining the properties of tangent linear equations, adjoint operators, and many other mathematical approximations of real-world problems.

It is the rise of more-and-more powerful computational devices after World War II that changed our way of thinking about what the solution to the mathematical formulation of a physical problem really is, that is, not necessarily an analytical expression but an algorithm for obtaining information about such a solution with prescribed accuracy. The improvement in observational methods—in the geosciences and elsewhere,

whether in vitro, that is, in the lab, or in vivo, that is, outdoors—has also contributed greatly to our appetite for going beyond linear approximation to model, simulate, understand, and predict the complexity of the phenomena under study.

The nonlinear way of thinking about problems, in the geosciences and many other sciences—physical sciences in general, biosciences, and socioeconomic sciences—still needs to operate within the circles of light projected into the night of our ignorance by a certain number of lampposts. These lampposts include the theory of dynamical systems, statistical mechanics, scale invariances, the theory of localized coherent structures, and several others. Some lampposts that have been added or whose light circle has expanded in the last decade or so are network theory and the theory of nonautonomous and random dynamical systems.

The remainder of this paper will examine some of these lampposts and their respective circles of light, following and thoroughly updating two decades later Ghil et al. (1991) and Ghil (2001). Clearly, the bounds on the length of the paper—combined with the author's tastes and other limitations—have affected the selection of topics and the length to which each one of them could be treated. Moreover, the author is not a historian of science and the paper does not claim, nor can anyone else, to provide a fully complete and accurate description of the rich web of influences among many researchers active in the fields upon which this review is touching, however lightly.

With these disclaimers being stated, let us proceed. In the next section, we outline with a broad brush how linear results provided first insights into the behavior of fluid motions, around the turn of the nineteenth into the twentieth century, and how nonlinear ones completed our knowledge after World War II.

Sections 3 and 4 examine in somewhat greater detail the dynamical systems and the scale invariance lamppost, respectively. Each section starts with a sketch of the basic concepts and methods, in sections 3.1 and 4.1, respectively; each then follows up with some key applications. Thus, in section 3.2 we discuss the mechanics of vacillation, multiple weather regimes in the atmosphere, and multiple flow regimes in the oceans, while in section 4.2 we cover succinctly fractals in dynamical systems, as well as scale invariance in general three-dimensional (3-D), two-dimensional (2-D), and geostrophic turbulence.

A few additional lampposts are examined in section 5, each subsection starting again with theoretical foundations, followed by selected applications. Section 5.1 covers network theory, including both topology and dynamics, in particular that associated with Boolean delay equations (BDEs); the applications illustrated are to earthquake and climate networks. In section 5.2 we discuss fluctuation-dissipation theory, outlining the classical theory for thermodynamic equilibrium, as well as the more recent out-of-equilibrium generalizations; applications to the climate system's response to natural and anthropogenic forcing are emphasized.

In section 5.3, we cover the extension of dynamical systems theory to nonautonomous and random dynamical systems; the applications are the stochastically perturbed Lorenz (1963a) model and the oceans' wind-driven circulation subject to time-varying wind stress. This subsection ends with an introduction to climate sensitivity and the use of Wasserstein distance to generalize the traditional concept of equilibrium sensitivity.

Section 6 presents two meanings of prediction as touchstones of progress in the nonlinear geosciences: (i) forecasting, that is, prediction in time of the quantitative realization of known phenomena and (ii) theoretical prediction of qualitatively new phenomena. The former meaning is illustrated by forecasting atmospheric and oceanic phenomena on longer and longer time scales, from days through seasons and on to several decades. The latter one is presented in the context of predicting an ice-covered Earth by simple energy balance models (EBMs) and leading to the current arguments about a snowball Earth. Section 7 concludes this review paper with a brief coda. All acronyms used in the text appear in Appendix A.

2. From Linear to Nonlinear Thinking: A Quick Review

A paradigmatic success of linear concepts and methods at the beginning of the twentieth century is the explanation by Lord Rayleigh (1916) of the striking patterns found in the thermal convection experiments of James Thomson (1882) and of Henri Bénard (1900). The word “paradigm” is used here advisedly in the sense of Thomas Kuhn (1962): it is easy to see how the transition from a linear—and for quite a while very successful—mode of thinking to a nonlinear one is not just an evolutive generalization but a genuine revolution.

In the next section, we will consider a few key traits of the nonlinear mode of thinking. In many applications to the physical sciences, like fluid dynamics, the linear mode involves linearizing the equation of motion about a suitably symmetric steady state, most often a state of rest (Rayleigh, 1916, p. 534). The stability of the resulting linear operator is examined and the spatial pattern of the most rapidly growing unstable mode can then be compared to observations. While Lord Rayleigh only examined a rectangular domain, subsequent work led to the study of convective rolls and hexagons as the most often occurring spatial patterns near equilibrium (e.g., Busse, 1978; Krishnamurti, 1973). It is interesting, though, that Rayleigh, (1916, pp. 529–530) does describe the irregular transitions between two types of flow regimes. Pursuing an explanation thereof was clearly beyond the reach of the linear methodology available to him.

Be that as it may, linear methodology led to many other successes during the first half of the twentieth century, in explaining flow patterns observed in the laboratory, in industry, and in nature. Thus, when we see parallel cloud streaks in the sky, we know that they are the result of either Rayleigh-Bénard or Kelvin-Helmholtz instability. Possibly the crowning success of this approach was the discovery of a truly 3-D instability of great importance for atmospheric and oceanic flows, namely, baroclinic instability, by Jule G. Charney (1947) and, independently, by Eric T. Eady (1949).

Charney's and Eady's results on baroclinic instability and variations thereupon managed to explain various features of the initial stages of development of midlatitude storms in the atmosphere and of mesoscale meanders in the oceans. But they could not explain the finite-amplitude interactions between separate storms nor help very much in predicting weather beyond 1–2 days. In fact, Eady, (1949, pp. 51–52) already had a pretty clear vision of the difference between theoretically identifying recognizable initial patterns in a storm's development and “the formidable task facing theoretical meteorology — that of discovering the nature of and determining quantitatively [sic] all the forecastable regularities of a permanently unstable (i.e., permanently turbulent) system.” It is here that the paradigmatic jump from linear to nonlinear concepts and methods has to occur.

3. The Dynamical Systems Lamppost

3.1. The Theory

The mathematical theory of dynamical systems deals with modeling the behavior of systems that evolve on long time scales, sufficiently long, that is, for assuming that solutions of the models exist for all times, from $-\infty$ to $+\infty$. This theory does not distinguish, in principle, linear from nonlinear systems but has much to say about the latter; it does not distinguish either between natural systems—whether physical, biological, or socioeconomical—and human-made systems, but we will be interested here in the natural ones. Some basic facts of nonlinear life are outlined below, from the dynamical systems perspective, following Ghil et al. (1991).

1. The equations of continuum mechanics are nonlinear. Surprisingly, many phenomena can be explained by linearization about a particular fixed basic state. Many more cannot; see section 2 above.
2. Behavior of solutions to the nonlinear equations changes qualitatively only at isolated points in phase-parameter space, called bifurcation points. Behavior along a single branch of solutions, between such points, is modified only quantitatively and can be explored by linearization about the basic state, which changes as the parameters change. That is, nonlinear dynamics is much like linear dynamics, only more so (Ghil & Childress, 1987; Lorenz, 1963a, 1963b).
3. Bifurcation trees lead from the simplest, most symmetric states, to highly complex and realistic ones, with much lower symmetry in either space or time or both. These trees can be explored partially by analytic methods (Jin & Ghil, 1990; Jordan & Smith, 2007) and more fully by numerical ones, such as pseudo-arclength continuation (Dijkstra, 2005; Legras & Ghil, 1985).
4. The truly nonlinear behavior near bifurcation points involves robust transitions, of great generality, between single and multiple fixed points (saddle-node, pitchfork, and transverse bifurcations), fixed points and limit cycles (Hopf bifurcation), limit cycles, and strange attractors (“routes to chaos”;; Eckmann, 1981; Guckenheimer & Holmes, 1983). As the complexity of the behavior increases, its predictability decreases (Ghil, 2001).
5. Behavior in the most realistic, chaotic regime can be described by the ergodic theory of dynamical systems. In this regime, statistical information similar to, but more detailed than for, truly random behavior can be extracted and used for predictive purposes (Eckmann & Ruelle, 1985; Ghil & Robertson, 2000; Mo & Ghil, 1987).

6. Chaos and strange attractors are not restricted to low-order systems. They can be shown to exist for the full equations governing continuum mechanics (Constantin et al., 1989; Temam, 2000). The detailed exploration of finite- but high-dimensional attractors is in full swing (Dijkstra, 2005; Ghil, 2017; Legras & Ghil, 1985).
7. Single time series (Takens, 1981) and single numbers derived from them (e.g., Grassberger, 1983) have been used to describe chaotic behavior. This very simple and straightforward use of a nonlinear concept has attracted considerable attention to deterministically chaotic dynamics, including in the geosciences (Nicolis & Nicolis, 1984; Tsonis & Elsner, 1988). The use of single time series, while exciting in theory, is not very promising when the series are short and noisy (Ruelle, 1990; Smith, 1988). The increasing availability of a large number of similar series at different points in space, combined with physical insight, is compensating more and more for the shortcomings of each individual time series in describing the complexity of many phenomena in the geosciences, as well as advancing their prediction (Ghil et al., 2002).

3.2. Some Results

The mechanics of vacillation. Two steps beyond linear theory, in the direction already outlined by Eady (1949), were taken by Edward N. (1963a, 1963b). The first one of the two was stimulated by the work on convection mentioned in section 2 above and revisited by Barry Saltzman (1962). This step yielded the paradigmatic strange attractor of Lorenz (1963a), too well known to be reviewed here yet another time; see Sparrow (1982), Guckenheimer and Holmes (1983), and Ghil & Childress, 1987 (1987, section 5.4). The contributions of this paper to the understanding of predictability in atmospheric sciences and in many other areas of the physical, biological, and socioeconomic sciences are covered in this Special Issue by Krishnamurthy (2019) and by McWilliams (2019).

Two previous examples of chaotic behavior in a low-dimensional system were particularly important, namely, the periodically forced Duffing (1918) and Van der Pol, 1920 (1920, 1926) oscillators; see, for instance, Guckenheimer & Holmes (1983, Chapter 2), as well as Cartwright and Littlewood (1945) and Pierini et al. (2018, Appendix A). Still, once the broader community of dynamical systems theorists (Li & Yorke, 1975) and mathematical physicists (McLaughlin & Martin, 1975) became aware of this third and most intriguing example of chaotic behavior, the contributions of Lorenz (1963a) and of his many followers played a key role in showing the road to understanding deterministic chaos in low-dimensional systems. The fractal dimension of the Lorenz (1963a) attractor will be treated in section 4.2 below.

The second step, taken by Lorenz (1963b), was going beyond the linear theory of baroclinic instability and was stimulated by the rotating-annulus experiments with differential heating of David Fultz (e.g., Fultz et al., 1959) and Raymond Hide (Hide & Mason, 1975, and references therein); see also Ghil et al. (2010). In this step, Lorenz (1963b) showed how to proceed from the initial baroclinic instability of Charney (1947), via successive bifurcations, to the so-called index cycle of atmospheric mid-latitude variability. Namias (1950) described this cycle of the zonal index as a recurrence of changes in intensity of the prevailing westerlies, with a rough periodicity of 4–6 weeks.

Lorenz, (1963b, Figure 3) reproduced key features of this phenomenon—such as the changes in strength, latitude, and meandering of the westerly jet—by associating them with the tilted-trough vacillation in the rotating annulus experiments. The corresponding bifurcation tree appears as Figure 5.8 in Ghil and Childress (1987).

Multiple weather regimes. Charney (1947) and Eady (1949) followed the linear approach outlined in sections 1 and 2 and assumed small perturbations about a stationary midlatitude state of zonally symmetric flow. But observational meteorologists knew already that predominantly zonal flow is only one of the midlatitudes' persistent states and that episodes of so-called blocked flow—with large deviations from zonality—can persist for fairly long times (e.g., Baur, 1947; Namias, 1968). “Long” here is defined as longer than the life cycle of a typical midlatitude storm, which is 5–7 days, while blocking events can last for up to a month (e.g., Dole & Gordon, 1983); see also Ghil & Childress, 1987 (1987, Figure 6.1).

Charney and DeVore (1979) studied a low-order barotropic model with merely three modes in a β -channel—that is, in a rectangular domain on a tangent plane to the sphere (e.g., Gill, 1982; Pedlosky, 1987)—that had two stable stationary solutions: one with features similar to zonal flow, the other resembling blocked flow; see the bifurcation diagram in Ghil & Childress (1987, Figure 6.5). Charney et al. (1981)

and Benzi et al. (1986) provided observational evidence for the existence of blocked-vs.-zonal bimodality in the Northern Hemisphere extratropics, while Mo and Ghil (1987) also found bimodality in the Southern Hemisphere extratropics. The latter bistability involved different amplitudes and phases of a dominant wavenumber-three, quasi-stationary wave; a third quasi-stationary pattern, of regional rather than hemispheric extent, was called by Mo and Ghil (1987) the Pacific-South-American (PSA) pattern.

Legras and Ghil (1985) showed that, using just 25 modes of a barotropic model on the sphere, one could go well beyond two stable fixed points, to obtain not only more realistic zonal and blocked flow but also stable limit cycles and deterministically chaotic behavior. In the latter regime, depending on the Rossby number Ro that determines the relative importance of the planet's rotation (see section 4.2 for further details), it is either a zonal, a blocked, or an intermittent regime that dominates. In the presence of intermittency, the relative time spent in zonal and blocked episodes changes smoothly as Ro increases Ghil & Childress (1987, Figure 6.14). Weeks et al. (1997, Figure 5B) used a barotropic rotating annulus with topography and found that the dependence of persistence times of zonal versus blocked flow on the experiment's Rossby number exhibited marked similarities to the numerical results of Legras and Ghil (1985).

The existence of several weather regimes in the Northern Hemisphere's atmosphere is statistically pretty well established now by a number of distinct clustering methods and their application to several data sets; see, for instance, Table 1 in Ghil et al. (2018), and references therein. Even so, the exact number of such regimes supported by the data, as well as their description and dynamical explanation, remains a matter of debate. Moreover, high-resolution numerical weather prediction (NWP) models—which are otherwise quite skillful at predicting weather a few days in advance—still have difficulties in predicting the onset of blocking and transitions between it and zonal flow (Dawson & Palmer, 2014).

Multiple flow regimes in the oceans. The horizontal extent of storms in the atmosphere and of eddies in the oceans is given by the Rossby radius of deformation R (Ghil & Childress, 1987; Gill, 1982; Pedlosky, 1987) that determines the so-called synoptic scale. Because of the differences in stratification between the two fluid media, $R_{oc} \simeq 100 \text{ km} \ll R_{atm} \simeq 1,000 \text{ km}$. Thus, when first discovered, oceanic eddies have been erroneously called “mesoscale eddies,” since 100 km is termed the mesoscale in the atmosphere. Be that as it may, the name has stuck (e.g., McWilliams, 2011).

While the diameter of oceanic eddies is much smaller than that of the atmospheric ones, their life cycle is much longer: months rather than days. Thus, low-frequency variability (LFV) in the oceans is on the scale of years-to-decades, while in the atmosphere it is subseasonal-to-seasonal, 10–100 days. In the oceans, one tends to distinguish between two types of causes of LFV: the wind-driven circulation and the thermohaline (THC) or meridional-overturning circulation. The former is predominantly in a horizontal plane, driven by atmospheric momentum fluxes, and contributes to the interannual LFV of the oceans, while the latter is predominantly in a meridional plane, driven by buoyancy fluxes and contributes to the interdecadal LFV (Dijkstra & Ghil, 2005).

Important contributions to the nonlinear understanding of oceanic LFV are roughly contemporaneous to, or even earlier than, the pioneering contributions of Lorenz, (1963a, 1963b) for the atmosphere. Henry Stommel (1961) obtained two stable stationary solutions in a simple two-box model of the THC. He was originally interested in the seasonal reversal of local THCs, such as in the Red Sea or the Eastern Mediterranean Stommel, (1961, p. 225) but did note on p. 228 that “One wonders whether other quite different states of flow are permissible in the ocean [...] and if such a system might jump into one of these with a sufficient perturbation. If so, the system is inherently fraught with possibilities for speculation about climatic change.” Speculations on this matter continue apace, and some of the relevant research is reviewed in Dijkstra & Ghil, 2005 (2005, section 3).

George Veronis (1963) considered the wind-driven ocean circulation in a rectangular basin on the β -plane, subject to time-independent wind stress, and truncating the expansion of the barotropic, single-layer stream function at four sine modes. He obtained two stable steady states, as well as a limit cycle for various parameter values.

Jiang et al. (1995) introduced a different expansion of the shallow-water equations in the same geometry, with an exponential multiplier in the zonal, x direction to allow for a western boundary current, as well as carrying out numerical integrations on an eddy-permitting grid with $\Delta x = \Delta y = 20 \text{ km}$. They obtained exact steady states, as well as exactly periodic solutions (Figure 1) for the numerical integrations that used

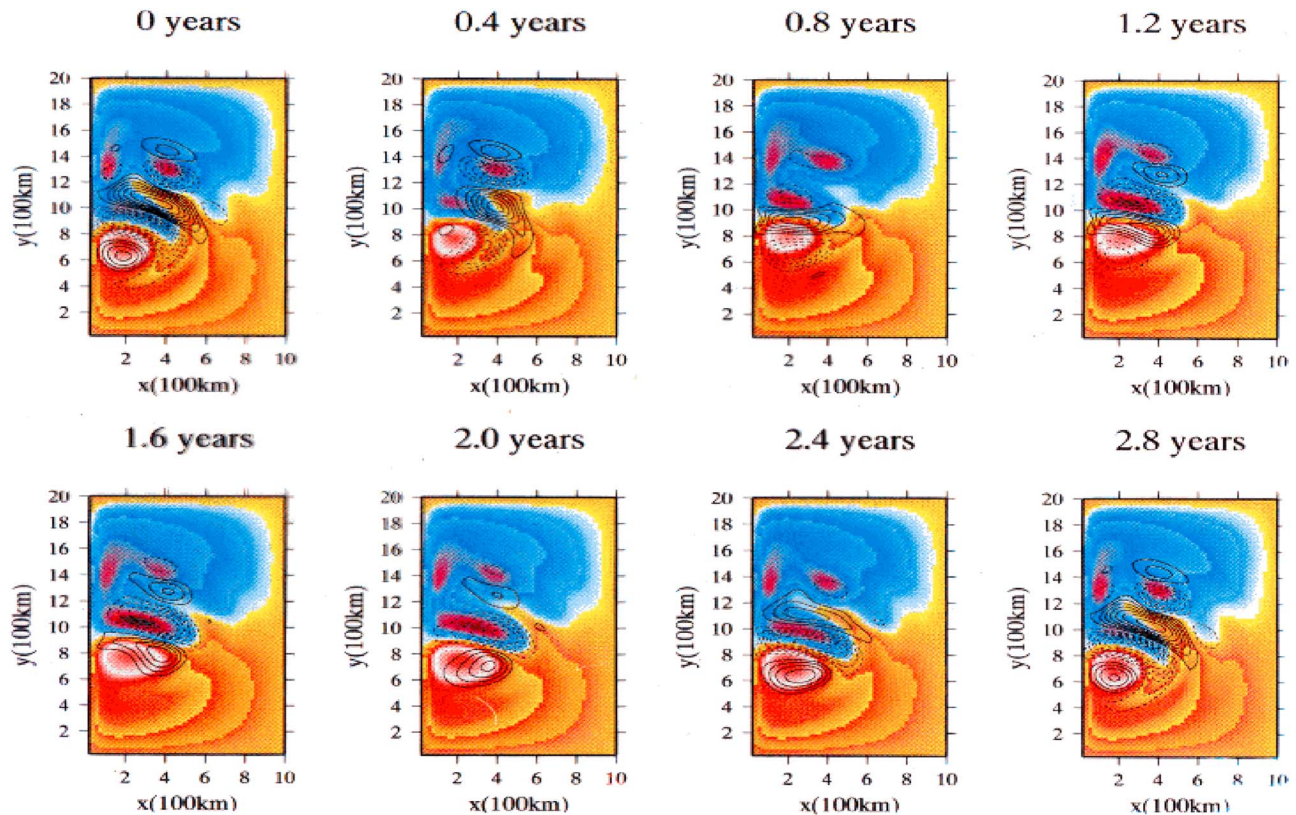


Figure 1. Snapshots from an exactly periodic relaxation oscillation of the Jiang et al. (1995) model; see also Figure 7 (black and white) there. Color indicates contours of the model's upper-layer thickness, with warm colors for the subtropical gyre and cold ones for the subpolar one; black lines indicate contours of potential vorticity, with a modified Rossby wave propagating across the basin. Courtesy of Shi Jiang.

15,000 grid variables. These authors also showed that the generation of the nearly mirror-symmetric steady states in the numerical integrations was well captured by the perturbed pitchfork bifurcation of their highly idealized, intermediate-order model.

The periodic solutions became more and more anharmonic and sawtooth shaped as the time-constant wind stress intensity was increased and finally led to aperiodic, intermittent solutions. This transition to chaos can be followed in Figure 2 via a homoclinic bifurcation for a quasi-geostrophic (QG) model with a resolution of $\Delta x = \Delta y = 10$ km. Dijkstra & Ghil (2005, section 2) provide further details on this particular model, as part of an entire hierarchy of increasingly detailed and realistic models that confirm its results, and many additional references. Concerning geostrophy and its effect on turbulent fluid behavior, see section 4.2 below.

Overall, the line of work outlined in the preceding paragraphs has provided fairly convincing evidence that intrinsic oceanic LFV, even in the absence of variable atmospheric forcing, is an important source of interannual climate variability. Detailed confrontation of model results with recent reanalysis data for both atmosphere and oceans supports these ideas, at least in the case of the North Atlantic basin (Groth et al., 2017), where this mechanism also provides a possible explanation of the North Atlantic Oscillation (NAO) and of its approximate 7- to 8-year periodicity. The situation for time-dependent wind forcing will be discussed in section 5.3.

Bifurcations and tipping points. In the applications covered herein, we have limited ourselves to classical bifurcations (e.g., Arnold, 2012; Guckenheimer & Holmes, 1983), which go back to the work of Leonhard Euler (1757) on buckling of a beam (e.g., Timoshenko & Gere, 1961). Recently, the interest in bifurcations in the geosciences has greatly increased due to the introduction of the concept of tipping points from the social sciences (Gladwell, 2000; Lenton et al., 2008). Clearly, a tipping point sounds a lot more threatening than a bifurcation point, especially when dealing with an earthquake or a dramatic and irreversible climate change.

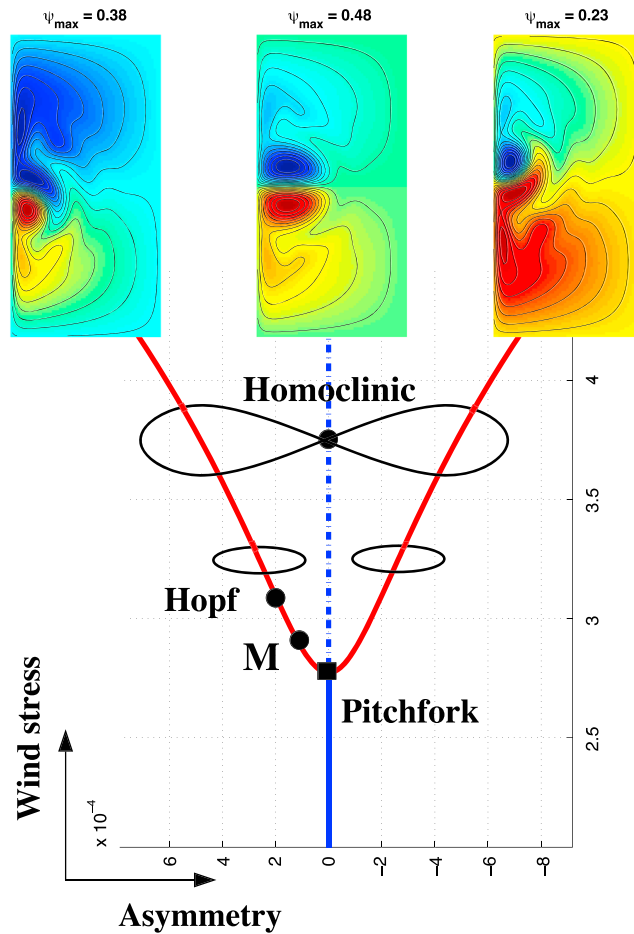


Figure 2. Generic bifurcation diagram for the barotropic quasi-geostrophic model of the double-gyre problem: the asymmetry of the solution is plotted versus the intensity of the wind stress τ . The stream function field $\psi = \psi(x, y)$ is plotted for a steady-state solution associated with each of the three branches; positive values in red and negative ones in blue. After Simonnet et al. (2005).

Aside from their rhetorical impact, though, tipping points generalize classical bifurcations in several important ways when considering open, rather than closed, systems. The physical difference between the former and the latter translates into the presence versus absence of explicit time dependence in the right-hand side or the coefficients of the governing system of evolution equations, be they low, high, or infinite dimensional.

Classical dynamical systems theory deals with closed systems, which are governed by models in which there is no explicit time dependence whatsoever. These models are called autonomous, and the time independence property plays a key role in the theory. For instance, given a system of two ordinary differential equations (ODEs) in the plane, uniqueness of solutions essentially prevents self-intersection of the orbits, which can only tend to fixed points or limit cycles. It takes either periodic forcing, as is the case for the Duffing or Van der Pol oscillator, or three autonomous ODEs in Euclidean 3-D space, as for the Lorenz (1963a) model, to get deterministically irregular, chaotic behavior.

The Earth system, though—as well as its subsystems, such as the solid Earth's core and mantle or its fluid envelopes' atmosphere and oceans—are open and exchange time-dependent fluxes of mass, energy, and momentum with each other and with outer space. It is high time, therefore, to start applying more systematically the theory of nonautonomous deterministic and of random dynamical systems to the whole Earth and to its various parts. This will be done in section 5.3 below.

At this point, let us just mention that there are three kinds of tipping points that have attracted recently considerable attention when studying open systems (Ashwin et al., 2012):

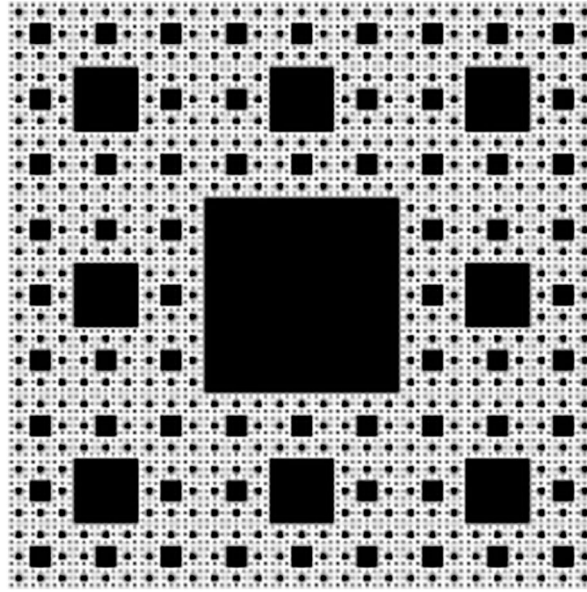


Figure 3. The sixth-level iteration for obtaining the Sierpiński carpet on the unit square $[0, 1] \times [0, 1]$. The carpet has topological dimension $d_T = 1$ but Hausdorff dimension $d_H \approx 1.893 < 2$. From Wikimedia, public domain.

- (i) B-Tipping or Bifurcation-due tipping: slow change in a parameter leads to the system's passage through a classical bifurcation;
- (ii) N-Tipping or Noise-induced tipping: random fluctuations lead to the system's crossing an attractor basin boundary; and
- (iii) R-Tipping or Rate-induced tipping: rapid changes lead to the system's losing track of a slow change in its attractors.

4. The Scale Invariance Lamppost

The light of this lamppost has to do with insights about patterns that appear to keep their spatial structure at increasing magnification. Such spatial patterns—like the Cantor set on the line and the Peano curve in the plane—were well known by the late nineteenth century (e.g., Sagan, 2012), but their pervasiveness in nature and connection to a system's evolution in time only became evident in the second half of the twentieth century.

4.1. The Theory

Probably the best known set with strange properties that arise by an iterative construction is the Cantor ternary set. Consider the closed unit interval $C_0 = [0, 1]$ of length $\ell_0 = 1$ on the real line \mathbb{R} and remove the open middle third $(1/3, 2/3)$, which leaves the set $C_1 = (C_0/3) \cup (2/3 + C_0/3) = [0, 1/3] \cup [2/3, 1]$ of length $\ell_1 = 2/3$. Removing inductively the open middle third of the two closed intervals left, then of the four ones left at the next stage and so on, one gets

$$C_n = \frac{C_{n-1}}{3} \cup \left(\frac{2}{3} + \frac{C_{n-1}}{3} \right), \quad (1)$$

of length $\ell_n = (2/3)\ell_{n-1} = (2/3)^n$. This construction is perfectly self-similar and scale invariant.

Clearly, $\ell_n \rightarrow 0$, so that the limit set $C_\infty = C$ has length $\ell_\infty = 0$. But the deep result is that there is a one-to-one correspondence between the points in the set C of zero Lebesgue measure and those in the unit interval C_0 ; that is, the two sets have the same uncountable cardinality $|C| = |C_0|$, which equals also the transfinite cardinality \aleph_1 of the real line itself. The former result was stated by Georg Cantor (1887) without proof; the modern proof is based on what became known as the Cantor-Schröder-Bernstein theorem, with Felix Bernstein and Ernst Schröder having almost simultaneously given two different proofs in 1897, as did Felix Dedekind. The 2-D generalization of the Cantor set in the plane \mathbb{R}^2 is called the Sierpiński (1916) carpet; see Figure 3.

Many mathematicians at the time were not comfortable with transfinite numbers nor with statements like the inequality $\aleph_0 < \aleph_1$, where \aleph_0 is the cardinality of natural, integer, and rational numbers, among other countable sets, nor did physicists in the late nineteenth century appreciate functions that were not continuously differentiable everywhere. This inequality and the absence of any cardinals between \aleph_0 and \aleph_1 depended on difficult issues raised by the axiomatization of mathematics (e.g., Suppes, 1972) that were not that palatable for most mathematicians and almost all physicists. This fact transpires even in Cantor's choice of journal for his 1887 paper, namely, a philosophical rather than a standard mathematical one.

The situation was as bad or worse with respect to functions that were not continuously differentiable anywhere. Bernard Bolzano and Augustin-Louis Cauchy had given early definitions of continuity in 1817 and 1823, respectively, and Karl Weierstrass had given the better known $(\epsilon - \delta)$ definition a few decades later. As discussed in section 2, physicists were extensively using ordinary and partial differential equations (ODEs and PDEs) around the turn of the nineteenth into the twentieth century and lack of continuous differentiability was considered a mathematical oddity of little use in studying natural phenomena.

Benoît Mandelbrot (1967) had an important role in stressing that this was not so. Hugo Steinhaus (1954) had already discussed what we now call fractional dimension, when Lewis Fry Richardson (1961) pointed out the “coastline paradox” and provided the polygonal method for correctly overcoming this paradox; see also Hunt (1998). Essentially, the length L of a coastline, river (e.g., Steinhaus's Vistula), or geographic border depends on the scale G used to approximate it by a polygon. Based on several examples available at the time, Richardson, (1961, Figure 17) proposed the approximation $L(G) = \kappa G^{1-D}$, where κ is a constant and $D \geq 1$ is the fractional dimension; the latter equals unity if the curve is smooth. Quite recently, Losa et al. (2016) found “[...] that among many fractal analysis techniques, only Richardson's method enables correct calculation of the length of an object's border or irregular line.”

The basic ingredients of Mandelbrot's development of fractal concepts and methods became available in the early twentieth century. First, Felix Hausdorff (1918) provided a generalization of dimension that allowed one to evaluate it for the kinds of odd sets we discussed above, cf. Figure 3; it is now called the Hausdorff dimension, and it can take on noninteger values. Second, the same year, Gaston Julia (1918) considered a class of iteratively defined sets in the complex plane \mathbb{C} that have the right oddity.

Speaking loosely, for a given holomorphic (i.e., complex analytic) function $f(z)$, with $z = x + iy$, the Julia set $\mathcal{J}(f)$ and the Fatou (1919) set $\mathcal{F}(f)$ are complements of each other, with $\mathcal{J}(f)$ being the set of points on which repeated iterations of $z \rightarrow f(z)$ diverge, while on $\mathcal{F}(f)$ these iterations behave similarly. In other words, f is regular on $\mathcal{F}(f)$ and chaotic on $\mathcal{J}(f)$. As for the Cantor set C above, we only outline here the simplest case, namely, that of quadratic polynomials, written as $f_c(z) = z^2 + c$, with $c \in \mathbb{C}$. It is this case that Benoît (Mandelbrot, 2013, and references therein) made famous in the late twentieth century.

For $c = 0$, the Julia set is simply the unit circle $\{z : |z| = 1\}$, and the two Fatou sets are its interior and exterior, with iterations that converge to 0 and ∞ , respectively. In general, though, the Julia set $\mathcal{J}(f_c)$ is much more complicated and Mandelbrot (1977) introduced the term “fractals” for such complicated sets. A beautiful illustration of the self-similarity that characterizes many fractals is given by the Mandelbrot set $\mathcal{M}(f)$, defined as the set of points c in the complex plane for which the iterates

$$\{z_{n+1}(c) = f(z_n; c); n = 0, \dots\}$$

stay bounded as n increases, when starting at $z_0 = 0$. The most often studied and cited case is that of $f(z; c) = f_c(z) = z^2 + c$.

While there is no definitive consensus on how best to define a fractal, there are two key ingredients: (i) a degree of self-similarity and (ii) a Hausdorff dimension d_H that exceeds the classical, topological dimension d_T . The rigorous mathematical definition of the latter is also laborious, but its integer values are obvious for the usual Euclidean spaces, namely, $d_T = n$ for \mathbb{R}^n ; the former is often an irrational number, although a “fractal dimension,” while often used, is an obvious misnomer: it is the set that is a fractal, while the dimension is a simple scalar in all cases, and a fraction in many.

Both Julia sets, defined for a fixed c as z varies, and Mandelbrot sets, defined for a fixed $z_0 = 0$ as c varies, have fascinating properties and there are interesting connections between the two. Peitgen and Richter (2013) provide both mathematical substance and beautiful illustrations on these topics. Figure 4 illustrates just one

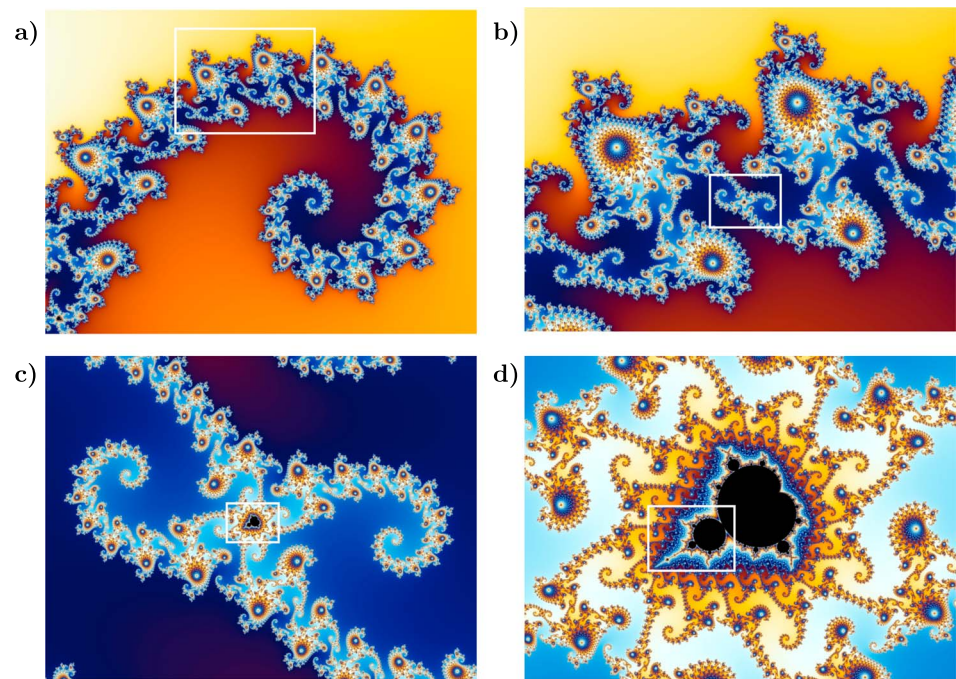


Figure 4. Mandelbrot set, with c_r on the abscissa and c_i on the ordinate. The white rectangles indicate the domain of the zoom in the next panel. Created by Wolfgang Beyer with the program *Ultra Fractal 3* (https://commons.wikimedia.org/wiki/File:Mandel_zoom_00_to_01.png); Steps 4–8 of the iteration are reproduced here as panels (a)–(d) of the figure, under the Creative Commons Attribution-Share Alike licence (<https://creativecommons.org/licenses/by-sa/2.5/deed.en>).

such case, but for this set, the scale invariance is more qualitative: things look roughly the same rather than exactly the same at different scales.

4.2. Some Results

Fractals in dynamical systems. A number of factors concurred in the second half of the twentieth century to greatly increase the circle of light of this lamppost, as well as the interest in it. First, there was the increase of interest in dynamical systems and their applications, as reviewed in sections 2 and 3 herein. Next, like in the case of dynamical systems, it was the great progress in computing power and storage capacity.

It is great fun computing Julia or Mandelbrot sets on your laptop, as it is computing the strange attractor of the Lorenz (1963a) model. Moreover, this attractor is a fractal for a broad range of parameter values, that is, when you drill through it perpendicular to the tangent manifold, anywhere except at the origin, you get a Cantor-like set.

Before discussing the dimension of this strange attractor, a few comments are in order on the concept in general, and on the role of this particular attractor in the general theory. A good overview is given by David Ruelle, (1995, pp. ix–xvii); the book also contains a collection of the author’s papers on the related topics of chaos, strange attractors and turbulence.

The concept of a strange attractor was introduced by Ruelle and Takens (1971a) and Ruelle and Takens (1971b) added to the former paper a list of references from the Soviet literature made available to them after the previous paper was published. Neither paper cites Lorenz (1963a) and, in fact, Ruelle, (1995, p. ix) specifically states that

“Based on a computer study, Edward Lorenz [3] identified in 1963 a time evolution with sensitive dependence on initial conditions (the Lorenz attractor). He also rediscovered Poincaré’s idea that weather predictions are limited by sensitivity to initial conditions. Just as Lorenz was unaware of Poincaré, physicists and mathematicians were largely unaware of the findings of Lorenz (a meteorologist) until the mid 1970’s.”

References [1] and [2] in the introduction to Ruelle (1995) are Hadamard (1898) and Poincaré (1908). Both these references were well known to mathematicians and physicists working on dynamical systems and their ergodic theory in the 1960s and 1970s (e.g., Smale, 1967). Note, by the way, that the journal in which Hadamard's work was published is the same as that of Julia (1918), 20 years later, whose work was discussed in section 4.1 above. It is McLaughlin and Martin (1975) and Li and Yorke (1975), already mentioned at the beginning of section 3.2, who made “physicists and mathematicians [aware] of the findings of Lorenz [in] the mid 1970's.”

This being said, it is time to return to the dimension of the fascinating Lorenz (1963a) attractor. For the standard nondimensional parameter values illustrated in the original Lorenz (1963a) paper—namely, the Rayleigh number $\rho = 28$, the Prandtl number $\sigma = 10$, and the wavenumber $\beta = 8/3$ —are $d_H = 2.06 \pm 0.01 > 2 = d_T$ and its volume is zero, as for the Cantor set. Please see, again, Sparrow (1982), Guckenheimer and Holmes (1983), and Ghil & Childress, 1987 (1987, section 5.4), as well as Krishnamurthy (2019) and McWilliams (2019) in this issue for further details.

While several metric dimensions have been defined for dynamical systems (e.g., Farmer et al., 1983), a particularly useful one is the Lyapunov dimension. It is given by the Lyapunov spectrum of the underlying system and is also called the Kaplan-Yorke dimension (Kaplan & Yorke, 1979):

$$d_{KY} \equiv k + \sum_{j=1}^k \frac{\lambda_j}{\lambda_{k+1}}; \quad (2)$$

here k is the maximum integer such that the sum of the k largest exponents is still nonnegative. We shall return to the Lyapunov spectrum in section 6 below. Leonov et al. (2016) obtained the following remarkable formula for the Lyapunov dimension d_{KY} of the global attractor of the Lorenz (1963a) model:

$$d_{KY} = 3 - \frac{2(\sigma + \beta + 1)}{\sigma + 1 + ((\sigma - 1)^2 + 4\rho\sigma)^{1/2}} < 3. \quad (3)$$

Dynamical systems and weak turbulence. Of course, it is one thing to describe numerically and study mathematically fractals in dynamical systems and quite another thing to do so in natural phenomena. As already indicated in section 1, the improvement in making and in analyzing observations, with their rapidly increasing number and accuracy, has also greatly accelerated the uses of scale invariance in the natural environment.

A particularly stimulating example is given by turbulence in general and by geophysical turbulence more specifically. Turbulent flow arises in many areas of engineering, as well as in nature, from blood flow to galactic evolution. Its presence and intensity is characterized by the Reynolds number $R \equiv UL/\nu$, where U , L , and ν are a characteristic velocity, length, and kinematic viscosity of the flow and the fluid: the higher U or L and the smaller ν , the more turbulent the flow.

Understanding and predicting turbulent behavior is probably the hardest problem in continuum physics. Compared to huge progress throughout the twentieth century in quantum and relativistic physics, progress in turbulence studies has been more moderate.

In fact, in the opening article of the *Annual Reviews of Fluid Mechanics*, Sydney Goldstein (1969) attributes to Sir Horace Lamb the following statement “I am an old man now, and when I die and go to Heaven there are two matters on which I hope for enlightenment. One is quantum electrodynamics, and the other is the turbulent motion of fluids. And about the former I am really rather optimistic.” The “old man,” of course, was a leader in fluid dynamics at the turn of the nineteenth into the twentieth century and the author of the Lamb (1932) book on which the generation of S. Goldstein, Ludwig Prandtl, and Theodor von Kármán had grown up. Goldstein's comment on this quote is, “Lamb was correct on two scores. All who knew him agreed that it was Heaven that he would go to, and he was right to be more optimistic about quantum electrodynamics than turbulence.” Goldstein's prediction still holds 50 years later, although we do mention some interesting glimpses of progress below.

Before addressing the application of scale invariance to various kinds of turbulence, it is important to touch upon the change in perspective brought by the application of dynamical systems ideas. The standard view of the onset of turbulence in fluids until the time of the Goldstein (1969) review was that of Landau and Lifshitz (1959). In this view, successive Hopf bifurcations lead to an increasing number of oscillatory modes

with rationally unrelated periodicities, which give rise to quasiperiodic and thus fairly irregular behavior in time (e.g., Hopf, 1948).

Ruelle and Takens (1971a) proposed, instead, that a much shorter bifurcation tree leads to what they called a turbulent or strange attractor. Until that time, bifurcations had mostly been studied for low-dimensional systems (e.g., Andronov et al., 1966). But a number of pioneering experiments with fluids convinced the community that a sequence of just a few bifurcations (cf. Eckmann, 1981) can lead to irregular, aperiodic behavior in continuous media. Some of these exciting developments are covered in Swinney (1978) and Ghil et al. (1985), and references therein.

It was in the next decade that fluid dynamicists realized that these transitions to, or the onset of, turbulence represent only the beginning of the story. Hence, the type of flows that resulted after traveling the roads to turbulence discussed so far were dubbed “weak turbulence” (e.g., Libchaber, 1985). Fully developed turbulence lay farther along the road, and at considerably higher Reynolds or Rayleigh numbers, depending on the nature of the flow, whether isothermal or thermally active (e.g., Benzi & Biferale, 2009; Ravelet et al., 2008).

Fractals in fully developed turbulence. Rapid technological progress still obliged engineers and other practitioners to find empirical results even in the absence of deeper understanding of the causes of turbulence and the behavior of turbulent flows. In particular, once the crucial role of boundary layers in mediating the transition between the fairly frictionless flow far from a wall and the necessity of a viscous fluid to be at rest at the boundary was understood, several empirical formulas were developed. Schlichting & Gersten, 2016 (2016, and earlier editions) are a good source for this important subfield of turbulent fluid dynamics.

Thus, assumptions about the phenomena at play that appear at first sight rather strong, along with dimensional analysis (e.g., Barenblatt, 1996), lead to the well-known “law of the wall.” Let U be the (nearly constant) velocity outside the boundary layer, τ_w the shear stress at the solid surface, y the distance perpendicular to the surface, $u_\tau = (\tau_w/\rho)^{1/2}$, with ρ the density of the fluid, μ its molecular viscosity, and $\nu = \mu/\rho$ its kinematic viscosity. The law is then given by $U/u_\tau = f(u_\tau y/\nu)$ and it holds for the “inner layer” $y \leq 0.2\delta$, where δ is the total thickness of the boundary layer.

Based on work variously attributed to Lev Landau in the former Soviet Union and to L. Prandtl and Th. von Kármán in the western literature, the form of the function f above is logarithmic, resulting in the log-law

$$\frac{U}{u_\tau} = \frac{1}{\kappa} \ln \frac{u_\tau y}{\nu} + C; \quad (4)$$

see Bradshaw & Huang, 1995 (1995, and references therein). Extensive experimental work shows that equation (4) holds for $\kappa \simeq 0.41$ and $C \simeq 5.0$, provided the pressure gradient parallel to the wall is not too large, within the region $30\nu/u_\tau \leq y \leq 0.1\delta$. The goodness of fit of the log-law above decreases as the pressure gradient increases and one approaches separation of the boundary layer.

Such semiempirical relations, based on physical approximations and dimensional analysis, served practitioners well. Still, there was an increasing need for fundamental understanding of the complexities involved in fully turbulent flows.

A truly major step forward was due to the development of the energy cascade concept and of the statistical theory of turbulence. In his pioneering study of NWP, L. F. Richardson, (1922, p. 66) formulated the key idea of a turbulent cascade via the verse “Big whirls have little whirls that feed on their velocity, and little whirls have lesser whirls and so on to viscosity—in the molecular sense.”

This idea was refined first by distinguishing between the largest scales in a fluid that are most energetic and are affected by the geometry of the domain, and the smallest ones, at which energy input from non-linear interactions and the energy drain from viscous dissipation are in exact balance. The latter have high frequency and are locally isotropic and homogeneous (e.g., Batchelor, 1953). In between these two scales, geometric and directional information is lost in the A. N. Kolmogorov (1941) inertial cascade, between the large scales L and the Kolmogorov scale ℓ_K , provided the Reynolds number R is sufficiently high.

The value of ℓ_K is given again merely by dimensional arguments and the physical assumption that the statistics of the small scales are universally and uniquely determined by the rate of energy dissipation ϵ and the kinematic viscosity ν , as $R \rightarrow \infty$,

$$\ell_K = (\nu^3/\epsilon)^{1/4}.$$

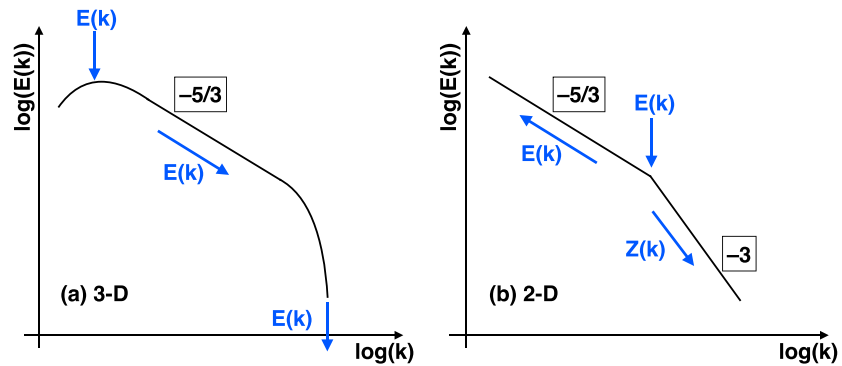


Figure 5. Energy and enstrophy cascades in (a) three-dimensional (3-D) and (b) two-dimensional (2-D) turbulence. The latter panel also characterizes the dual cascades in quasi-geostrophic turbulence. Courtesy of Niklas Boers.

Between L and ℓ_K , instabilities break up the larger eddies into smaller ones that interact nonlinearly, while viscous effects are negligible. Once more, these assumptions and dimensional analysis lead—for scalar wavenumbers $k = 2\pi/r$ and $L > r > \ell_K$, where $r = |\mathbf{r}|$ and \mathbf{r} is the distance in the physical space \mathbb{R}^3 —to the kinetic energy spectrum $E = E(k)$, namely,

$$E(k) = C\epsilon^{2/3}k^p, \quad (5)$$

with $p = -5/3$ and C a presumably universal constant.

Frisch (1995) presents this statistical theory of 3-D turbulence elegantly and reviews the experimental evidence, which confirms broadly the theory. This so-called direct energy cascade appears in Figure 5a. There are two related difficulties, though. First, to cite again Goldstein (1969), “[...] distinguished mathematical statisticians, some of whom had hopes of contributing to the theory of turbulence, [when] they saw the physical, rather than mathematical, nature of Kolmogorov’s contribution [...] decided that such research was not for them.” Indeed, to this day—and in spite of considerable progress in the mathematical theory of the Navier-Stokes equations that govern fluid dynamics (e.g., Temam, 2001)—there is no rigorous derivation of the Kolmogorov ($-5/3$) law.

Second, the Kolmogorov (1941) theory implicitly assumes that 3-D turbulence is statistically self-similar at different scales in the inertial range. Thus the flow velocity increments $\delta\mathbf{u}(r) = \mathbf{u}(x+r) - \mathbf{u}(x)$, when scaled by $\lambda > 0$, should behave as $\delta\mathbf{u}(r) \simeq \lambda^\beta \delta\mathbf{u}(r)$, with β independent of r , where \simeq stands for equality in distribution. It follows that the structure functions of order n , that is, the n^{th} -order statistical moments of the flow velocity increments $\delta\mathbf{u}$, should scale as

$$\langle (\delta\mathbf{u}(r))^n \rangle = C_n (\epsilon r)^{n/3}, \quad (6)$$

where the brackets denote the statistical average, and the C_n are universal constants.

More generally, given $1 < |p| < 3$ in equation (5), one can show that the second-order structure function, that is, $n = 2$ in equation (6) behaves like r^{p-1} . Since the latter is easier to measure accurately, $\langle (\delta\mathbf{u}(r))^2 \rangle \propto r^{2/3}$ implies that $p = 5/3$, confirming Kolmogorov (1941) theory. In fact, experimental differences are of the order of 2% (Mathieu & Scott, 2000). So far, so good.

Higher-order structure functions, though, deviate more and more from the scaling predicted by equation (6), as they become a sublinear function of n , and the constants C_n are far from universal, according to both laboratory and numerical experiments. The main reason for the observed deviations is the lack of homogeneity in the turbulent flow field, in either time or space; this feature of turbulence is referred to as intermittency and Mandelbrot (1969) highlighted its role: he conjectured that, as $R \rightarrow \infty$, the dissipation of the energy, far from being uniform, tends to concentrate on a fractal set with $d_H < 3$. Lagrangian coherent structures play an important role in reducing dissipation, producing intermittency in turbulent flows, and increasing their predictability (e.g., Haller, 2015).

Geophysical turbulence. Large-scale atmospheric and oceanic flows are characterized by the key role of rotation and shallowness (e.g., Ghil & Childress, 1987; Gill, 1982; Pedlosky, 1987). The theoretical study of such

flows is referred to as geophysical fluid dynamics (GFD) and an important tool in this study is the QG approximation; see Ghil & Childress (1987, Chapter 4) for a succinct introduction.

Shallowness is due to the small aspect ratio $\delta \equiv H/L \ll 1$, where H is the characteristic height—with $H \simeq 10$ km in the atmosphere and even smaller in the oceans—and L the characteristic horizontal extent, with $L \simeq 10^3$ km in the atmosphere and $L \simeq 10^2$ km in the oceans. The dominant role of planetary rotation is due to the smallness of the Rossby number $Ro \equiv U/fL \ll 1$, where U is a characteristic horizontal velocity, $f = 2\Omega \sin \phi$ is the Coriolis parameter that measures the local angular velocity, while Ω is the planet's angular velocity of rotation around its axis and ϕ the latitude.

QG flows are hydrostatic, that is, vertical accelerations are negligible due to the flows' shallowness, and they are dominated by geostrophic balance between the Coriolis force and the pressure gradient. These two features result in QG flows being 2-D to a good first approximation, which suggests that geostrophic turbulence should also have 2-D features (e.g., Cushman-Roisin & Beckers, 2011; McWilliams, 2011; Salmon, 1998). We start by rapidly reviewing the differences between 2-D and 3-D turbulence.

The key difference is the existence of two quadratic invariants, enstrophy and kinetic energy, rather than energy alone; see the references in Charney, (1971, pp. 1087-1088), with enstrophy Z being the mean-squared vorticity. In 3-D turbulence, the conservation of the kinetic energy $E(k)$ leads to the direct cascade from large to small scales, cf. equation (5), as illustrated in Figure 5; the slope of the $E(k)$ spectrum over the inertial range $L \leq k \leq \ell_K$ equals approximately $-5/3$.

In 2-D turbulence, the existence of the two separate, positive-definite quadratic invariants, kinetic energy E and enstrophy $Z(k)$, leads to two cascades. Indeed, Fjørtoft (1953) showed that an energy transfer from k to $k + \Delta k$ must, to conserve $Z(k)$, be accompanied by a larger transfer of energy to $k - \Delta k$; this follows, essentially, from $Z(k) \propto k^2 E(k)$. Based on this crucial fact, Kraichnan (1967) showed that, in 2-D turbulent flows, there are two inertial ranges: one with a reverse energy cascade and zero enstrophy flux, between L and L_* , the other with a direct enstrophy cascade and zero energy flux, between L_* and ℓ_K . The slope of the energy spectrum in the former is $(-5/3)$, and it is (-3) in the latter, as illustrated in Figure 5b.

Charney (1971) noted atmospheric observations (e.g., Wiin-Nielsen, 1967) and numerical simulations (e.g., Manabe et al., 1970) of a k_z^{-3} energy spectrum, where $7 \leq k_z \leq 20$ is the zonal wavenumber, with a corresponding range of linear scales from 1,500 to 4,000 km. He emphasized, though, that the previously accepted analogies between 2-D and QG flows are not really sufficient to argue for a similarity of the turbulent physics, given the fact that the baroclinic instability that injects energy at $L_* \simeq 10^3$ km is highly 3-D.

Charney (1971) argued that a deeper reason for the k_z^{-3} spectrum is the possibility, in geostrophic turbulence, to combine its two quadratic invariants into a single one, which he termed “pseudo-potential vorticity,” following previous work of his own. In 1971, no sufficiently accurate observations or simulations were available for distinguishing among several hypotheses for the atmospheric spectrum beyond $k_z = 20$. As such observations did become available, Nastrom and Gage (1985) showed that (i) all the way down to 2.6 km, there are no spectral gaps; and (ii) in fact, the k_z^{-3} spectrum associated with the k_z^{-3} enstrophy cascade is followed by yet another $(-5/3)$ slope, as the flow becomes 3-D at the smallest scales; see Figure 6.

Subsequent work, reviewed by Rhines (1979), Salmon (1998), and McWilliams (2011), among others, has greatly refined understanding of both atmospheric and oceanic turbulence, including the role of intermittency in deviating from simple $-5/3$ and -3 laws. The interest of GFD practitioners for 2-D turbulence, combined with the computationally much easier task of carrying out high-resolution, high- R calculations in 2-D led to an important discovery linking localized coherent structures with intermittency and increased predictability (Legras et al., 1988; McWilliams, 1984).

These structures were shown to be stable nonlinear solutions of the 2-D Euler equations. They represent, therewith, a depletion of nonlinearity in the turbulent flow field, locally inhibit the direct enstrophy cascade, and can survive for long times. As a result, the predictability time of large-scale dynamics increases, being no longer limited as much by the small-scale fluctuations; see the recent review of Haller (2015).

Sakuma and Ghil (1991) also reviewed some of the pertinent GFD literature, as well as proving stability for such localized coherent structures in the shallow-water equations, and emphasizing the analogies with magnetohydrodynamics (MHD). These analogies arise from the similarity between the role of the magnetic field vector \mathbf{B} in the latter and the angular rotation vector Ω in GFD (e.g., Ghil & Childress, 1987; Hide, 1989).

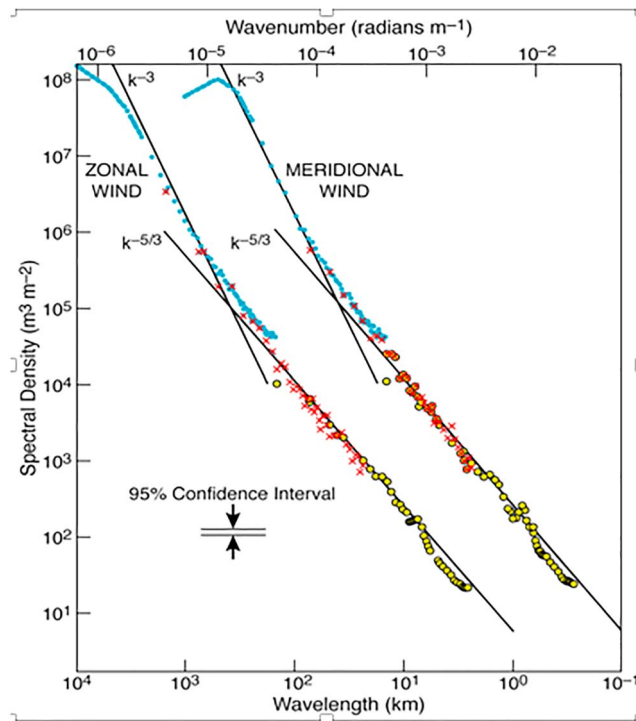


Figure 6. Wavenumber spectra of zonal and meridional velocity composited from three groups of flight segments of different lengths; these groups were selected from over 6,000 commercial aircraft flights. The three types of symbols (blue, red, and yellow) show results from each group. The least squares-fitted straight lines indicate slopes of (-3) and $(-5/3)$. The meridional wind spectra are shifted one decade to the right for greater legibility. The actual observational results show the typical deviations from straight lines in log-log coordinates. After Nastrom and Gage (1985). ©American Meteorological Society; used with permission.

Helicity \mathbf{H} is an additional quadratic invariant in both 3-D and 2-D turbulence (Chorin, 2013, and references therein), but it is not sign-definite and hence does not have the same effect as enstrophy on balancing energy transfers. Still, it does give rise to both inverse and dual cascades, which are important in GFD as well as in MHD. Helicity dynamics and bidirectional cascades are discussed in this issue by Pouquet et al. (2019). A particularly important application is to astrophysics in general and to the solar wind in particular (e.g., Pouquet et al., 2017).

Dubrulle (2019), largely based on recent very high-resolution direct numerical simulations (DNSs) of 3-D flows, has pointed out that the homogeneity assumptions of the Kolmogorov (1941) scaling break down at the small-scale end ℓ_K of the energy cascade. To account for this loss of symmetry, she proposes a novel approach to fully developed turbulence, in which the singularities introduced by Onsager (1949) play a key role. Once again, this is but the beginning of a road but it is a promising one.

5. A Few More Lampposts

So far we have covered, to the extent allowed by the constraints of this special issue, some fundamental concepts, methods, and results of dynamical systems theory in section 3 and of scale invariance in section 4. We will sketch now, even more briefly, the skeleton of three additional lampposts that increasingly are helping shed some light on nonlinear effects in the geosciences.

5.1. The Network Lamppost

We live in a world that is more and more dependent on networks of computing devices, as well as of people. Network theory thus is playing a bigger role in both understanding and modifying this world. Its applications extend to a rapidly growing number of areas, which include of course the geosciences.

Arguably, it is the Burridge and Knopoff (1967) model of friction along a fault that is the first and still one of the most important models of this kind in the geosciences. The model consists of a string of blocks connected by springs and can also be thought of as a modification of the Fermi et al. (1955) model with differing

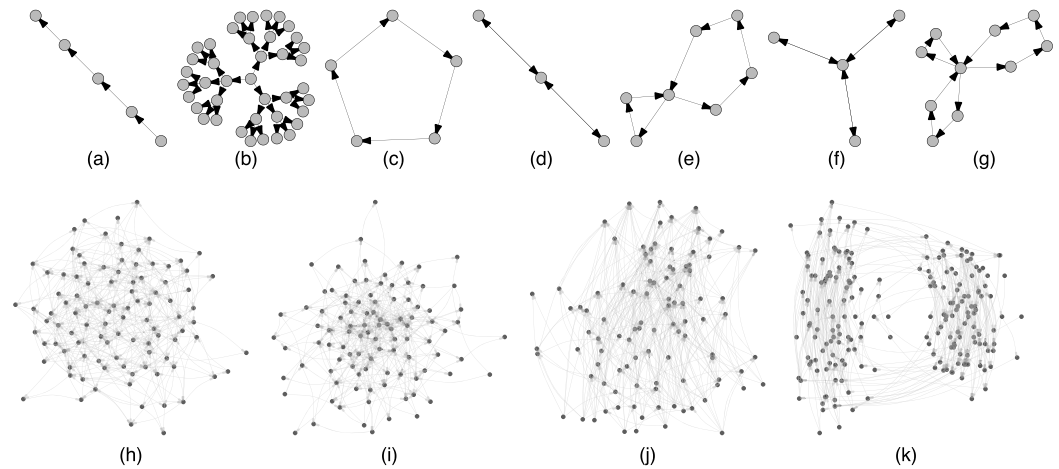


Figure 7. Schematic diagram of the network classes studied by Colon and Ghil (2017). Simple network motifs: (a) linear networks; (b) trees; (c) isolated loops; (d and e) two interacting loops, connected through a pivotal node; (f and g) three interacting loops. More complex classes of directed graphs, with $n = 100$ nodes and connectivity $c = 4$: (h) directed Erdős-Rényi (ER) networks; (i) scale-free networks with the specific, production-network distribution of in- and out-degree based on the Fujiwara and Aoyama (2010) data set; (j) random acyclic networks in which production moves upward; and (k) a network of two interdependent RA networks—in the network at left, production moves upward, while it moves downward in the one at right. Reproduced from Colon and Ghil (2017). Economic networks: heterogeneity-induced vulnerability and loss of synchronization, *Chaos*, 27, 126703, doi: 10.1063/1.5017851, with the permission of AIP Publishing.

nonlinear spring laws and the addition of nonlinear friction forces. It provided an understanding of the gradual accumulation and sudden release of potential energy associated with slow preseismic buildup and rapid displacement along an earthquake fault. The Burridge-Knopoff model, by its simple-model explanation of a baffling phenomenon, played a role in nonlinear solid-Earth studies that resembles that of the Lorenz (1963a) model in nonlinear atmospheric studies.

Network theory. More generally, network theory is a field of graph theory. A graph is an object with nodes that are connected by edges. The nodes and edges have certain attributes, for example, the physics at each node may be described by an ODE, while the link between two nodes may correspond to couplings between their ODEs. Such a network could then correspond to the method of lines being applied to a PDE (e.g., Schiesser, 2012).

A much simpler network could be a geometrically linear one, each of its nodes having an identical Boolean expression attached to it while being instantaneously connected to neighboring nodes. Such a network is called a cellular automaton (e.g., Von Neumann, 1951; Wolfram, 1983). For illustration purposes, Figure 7 shows a number of network classes recently studied by Colon and Ghil (2017).

A graph may be undirected, meaning that there is no distinction between the two nodes associated with each edge, or its edges may be directed from one node to another. The latter can be the case of river networks (Zaliapin et al., 2010, and references therein), supplier-producer networks (e.g., Colon & Ghil, 2017; Fujiwara & Aoyama, 2010), and many others (e.g., Albert & Barabási, 2002; Newman, 2010). A good example of the former is an Ising model on a 2-D lattice in statistical mechanics (e.g., Onsager, 1944) or a forest fire model of lesser (Malamud et al., 1998) or greater (Spyratos et al., 2007) complexity.

The topology of a network can be described by its adjacency matrix $\mathbf{A} = (a_{ij})$, where the entry a_{ij} equals 1 or 0 depending on whether an edge does exist between the nodes i and j or not. Much of network theory concentrates on various topological features, and on measures of centrality (Albert & Barabási, 2002; Newman, 2010, and references therein). Each of these measures aims to rank nodes by their importance, and they differ in how this importance is defined.

The simplest measure of centrality is the number of edges that it participates in, which is called the degree k . For directed graphs, one also distinguishes between the in- and out-degree. The distribution of degrees can be uniform, for example, $k \equiv 1$ for either a linear graph or a simple cycle and $k \equiv 2$ for a braid (e.g., Coluzzi et al., 2011); it can be fully connected, $k \equiv N - 1$, where N is the number of nodes; it can be fully

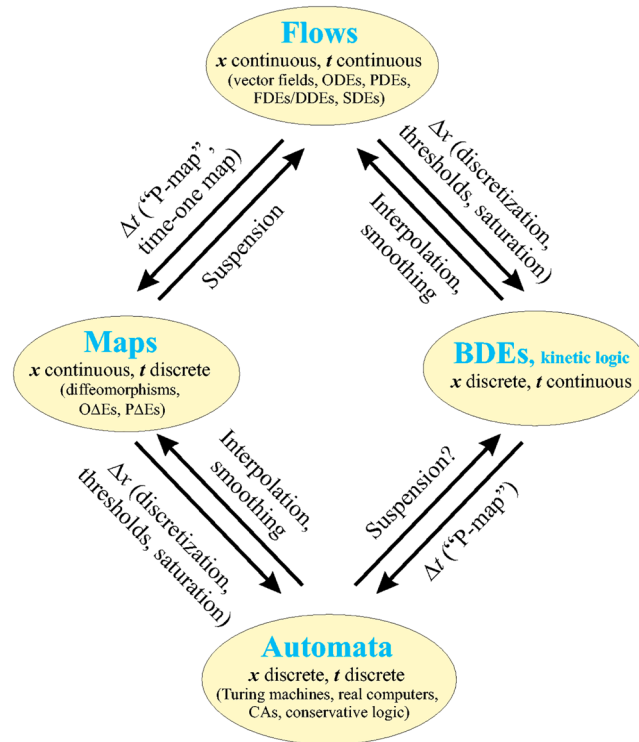


Figure 8. Schematic diagram of the distinct classes of dynamical systems, in terms of the state x and time t . Note the links: the discretization of time t can be achieved by the Poincaré map (P-map) or a time-one map, leading from *Flows* to *Maps*. The opposite connection is achieved by suspension. To go from *Maps* to *Automata* one has to discretize the station and smoothing lead in the opposite direction. Similar connections lead from *BDEs* to *Automata* and to *Flows*, respectively. Please see the glossary in Table A1 for acronyms. Modified after Mullhaupt (1984). ODE = ordinary differential equation; PDE = partial differential equation; FDE = functional differential equation; DDE = delay differential equation; SDE = stochastic differential equation; BDE = Boolean delay equation.

random, in which case the mean degree is $z = \bar{k} > N/2$; or it can be scale-free, that is, it obeys a power law, with $p(k) \simeq k^{-\alpha}$, with $\alpha > 0$.

The dynamics on a network depends on the mathematical description of the state of each node, its set of linked neighbors, and on the nature of the links, that is, on the coupling between the nodes. The state of each node can be described by a time series of real- or Boolean-valued variables; such time series, in turn, can either be provided by observations or be the result of evolution equations, be they systems of ODEs, PDEs, or of Boolean equations. The links, as previously mentioned, can be directed or not; they can also change in time in an evolving network.

Network applications. I: BDEs. We will give here an application to earthquake modeling and prediction. First, we introduce the framework of BDEs to describe the state of the nodes and the nature of the links.

A system of BDEs is a semidiscrete dynamical model with Boolean-valued variables that evolve in continuous time (Dee & Ghil, 1984; Ghil & Mullhaupt, 1985). The place occupied by BDEs in the world of dynamical systems is illustrated in Figure 8.

Systems of BDEs can be classified into conservative or dissipative, in a manner that parallels the classification of ODEs or PDEs. Solutions to certain conservative BDEs exhibit growth of complexity in time; such BDEs can be seen therefore as metaphors for biological evolution or human history. Dissipative BDEs are structurally stable and exhibit multiple equilibria and limit cycles, as well as more complex, fractal solution sets, such as Devil's staircases and "fractal sunbursts" (Ghil et al., 2008, and references therein).

More generally, Figure 8 raises the question of which one of the various types of dynamical systems therein apprehends best the complexities of the world surrounding us? Clearly, the amount of detail provided by

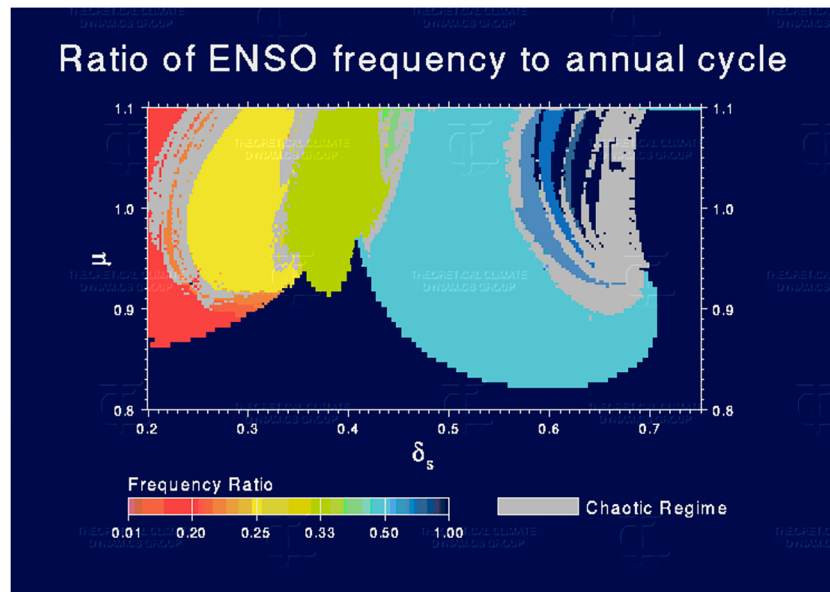


Figure 9. Regimes of subharmonic, frequency-locked and chaotic solutions in the (μ, δ_s) parameter plane; here μ is the local ocean-atmosphere coupling parameter and δ_s is an ocean mixed layer parameter that determines the model's intrinsic periodicity, in the absence of the annual cycle. Black areas represent regions where no interannual signal is present. Color scale represents the frequency ratio of the interannual oscillation to the annual cycle in regimes that are frequency locked; for example, 0.25 indicates one ENSO cycle every 4 years, 0.222 indicates two ENSO cycles repeating every nine years. Chaotic regimes are plotted in gray. Courtesy of Fei-Fei Jin. ENSO = El Niño/Southern-Oscillation.

each increases as we move from the *Automata* at the bottom to the *Flows* at the top of the rhomboid in the figure.

Thus, one level at which one can read the figure is as an illustration of the hierarchy of models discussed further in section 6. But there is also another way of reading it. In fact, each one of the downward-pointing arrows between a class of models and an adjacent one below it represents a perfectly self-consistent simplification, obtained as one discretizes either time t or space x . We all know how to obtain an ordinary or partial difference equation (OΔE or PΔE) from an ODE or PDE respectively, by discretizing time. The extent to which the solutions of the OΔE so obtained converge to those of the corresponding ODE depend on certain stability and consistency properties of the ODE's right-hand side (e.g., Isaacson & Keller, 2012).

In the case of a P-map, topological properties are preserved as one goes from a *Flow* to a *Map*, and maps are easier to study. Under certain technical assumptions dealing with smoothness and one-to-oneness, one gets most of what one wants from studying the map, since the suspension that goes back from the *Map* one has studied to the *Flow* can be proven to have the right properties. For instance, a periodic solution of the *Flow* will appear as a point in the *Map* and vice versa.

Can similar equivalence results be proven for other pairs of arrows in Figure 8? There exists numerical evidence, at least, to suggest that it might be true under suitable circumstances. Two such examples of, at least partial, equivalences are given below.

Saunders and Ghil (2001) provided a thorough BDE treatment of the El Niño/Southern-Oscillation (ENSO) mechanism postulated by J.Bjerknes (1969). Their Figure 7 of the “Devil’s bleachers” shows the dependence of the model ENSO’s periodicity on two model parameters that characterize the wave propagation along the equator and the local ocean-atmosphere heat exchanges, respectively; see also Ghil et al. (2008, Figure 6). The projection of the latter 3-D axionometric plot on its 2-D parameter plane is strikingly similar to Figure 9 herein.

This similarity is the first example of good numerical correspondence between two adjacent vertices of the rhomboid in Figure 8, since the “Devil’s terrace” in Figure 9 is based on the intermediate model of Jin et al. (1994, 1996). The latter model is governed by a system of nonlinear PDEs in one space dimension, namely,

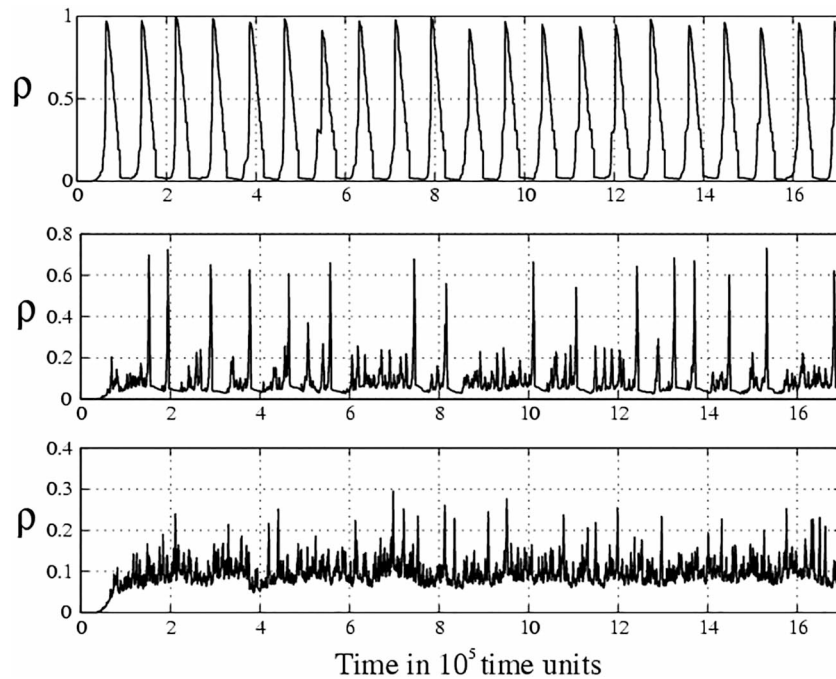


Figure 10. Three seismic regimes in the internal dynamics of the Boolean delay equation model, for a tree depth of $L = 6$, that is, for $n = 1\,093$ nodes. The panels show the density $\rho = \rho(t)$ of broken elements in the system. See Figures 7 and 8 in Zaliapin et al. (2003a) for loading and healing parameter values and other details. (a) Regime **H**, (b) Regime **I**, and (c) Regime **L**. Note the difference in vertical scale for the three panels. Reproduced from Zaliapin et al. (2003a) with kind permission of Springer Science and Business Media.

longitude along the equator, with the parameters μ and δ_s that appear in Figure 9 here; the two play a roughly similar role in the PDE model to that of the two parameters, local and global, in Ghil et al. (2008, Figure 6).

The early applications of BDEs to the climate sciences only used small systems of a few variables (e.g., Darby & Mysak, 1993). The first BDE application on a network was to a very simple model of seismic activity. The model consists of a ternary tree with a direct cascade of loading from a top node that represents a major plate, down to smaller and smaller plates. This direct cascade collides with an inverse cascade of failures that starts with the bottom nodes and travels up to larger and larger plates, possibly all the way to the top, depending on the delayed effects of healing (Zaliapin et al., 2003a, 2003b, and references therein).

Clearly, to analyze extensively and systematically systems of 3^L ODEs would be fairly prohibitive, even for a tree depth L as small as 6 or 7. Fairly surprisingly, though, the BDE model could be easily analyzed as a function of the loading and healing parameters, yielding the three well-known seismic regimes of high (**H**), low (**L**), and intermittent (**I**) seismicity, as shown in Figure 10.

The three regimes are characterized, respectively, by the following key features:

- H:** a cyclostationary behavior, with the maximum earthquake intensity reached on every cycle;
- I:** a highly intermittent behavior, with irregular intervals between major earthquakes and high, but not necessarily maximum intensity of the latter; and
- L:** a fairly low and nearly constant level of white noise-like seismic activity overall.

These features are present in observations (e.g., Romanowicz, 1993; Press & Allen, 1995), as well as in much more detailed and sophisticated models (Ben-Zion, 2008, and references therein). On the whole, it is the intermittent behavior that is most widespread, but a particular region can also change regime over time, as parameter values that affect the collective behavior of earthquakes and faults change. This is the second numerical example of at least partial equivalence between a *BDE* model and a *Flow*.

Network applications.II: Teleconnections and centrality. A very different network-theoretical setting was applied to climatic variability, and we discuss it now very succinctly herein, following Tsonis and Swanson (2008) and Donges et al. (2009). The idea that meteorological, oceanographic or coupled climatic variabil-

ity might involve “centers of action” that are widely separated in space goes back to Hildebrandsson and Teisserenc de Bort (1898) and to G. Walker’s “teleconnections” between them (Walker & Bliss, 1932). The statistical and dynamical study of such teleconnections engaged many important figures in the history of these disciplines over the last century (Bjerknes, 1969; Hoskins & Karoly, 1981; Wallace & Gutzler, 1981).

One of the main approaches used by A. A. Tsonis and colleagues (e.g., Tsonis et al., 2007), as well as by the groups around J. Kurths (e.g., Donges et al., 2009) and around S. Havlin (e.g., Gozolchiani et al., 2011), was labeled complex networks (CNs) and essentially consists in identifying the strongest correlations among time series at different locations. Boers et al. (2013) review relevant climate network literature and provide an application to the South American Monsoon System and to the spatial patterns associated with synchronization of extreme rainfall events; see also Boers et al. (2019) for a global analysis of extreme-rainfall teleconnections.

Many of the dynamical studies of the atmosphere’s LFV that involve teleconnections have used the highly simplified geometry of a so-called β -channel with periodicity in longitude and solid walls along parallels to the north and south of the channel, away from both the North Pole and the equator (Ghil & Childress, 1987; Pedlosky, 1987); see also section 3.2 herein. (Colon & Ghil, 2017, and references therein) showed that signal propagation in networks with distinct topologies in the plane can have very different properties; these properties are quite likely to be entirely different, in turn, from those of networks on the sphere. It is the latter that are most relevant to dynamical studies on a spherical domain, whether linear (e.g., Hoskins & Karoly, 1981) or nonlinear (e.g., Legras & Ghil, 1985). Thus, BDE models in such geometrically different settings as shown in Figure 7 here, on the plane and on the sphere, might complement or even guide further network-based investigations of teleconnections and climate variability.

5.2. The Fluctuation-Dissipation Lamppost

Fluctuation-dissipation theory (FDT) has its roots in the classical theory of statistical mechanics of many particle systems in thermodynamic equilibrium. The idea is very simple: the system’s return to equilibrium will be the same whether the perturbation that modified its state is due to a small external force or to an internal, random fluctuation (e.g., Kubo, 1966, and references therein). We outline below the simplest cases, and point to the generalization to systems out of equilibrium, such as the climate system or a network of seismic faults.

FDT. Like so many other ideas in the physical sciences, FDT goes back to Einstein and his *Annus mirabilis*, 1905. Einstein (1905) formulated the problem of the Brownian motion of a large particle immersed in a fluid formed of many small ones as follows. The presentation here follows Ghil & Childress, 1987 (1987, section 10.3), where further details can be found.

Consider the large particle as moving on a straight line with velocity $u = u(t)$, subject to a random force $\eta(t)$ and to linear friction $-\lambda u$, with coefficient λ . The equation of motion is

$$du = -\lambda u dt + \eta(t). \quad (7)$$

The random force $\eta(t)$ is assumed to be a “white noise”; that is, it has mean zero $\mathcal{E}[\eta(t; \omega)] = 0$ and auto-correlation $\mathcal{E}[\eta(t; \omega)\eta(t+s; \omega)] = \sigma^2 \delta(s)$, where $\delta(s)$ is a Dirac function, σ^2 is the variance of the white noise process, ω labels the realization of the random process, and \mathcal{E} is the expectation operator, which averages over the realizations ω . Alternative notations for the latter are the overbar, in climate sciences, and the angle brackets, in quantum mechanics, $\mathcal{E}[F] := \bar{F} := \langle F \rangle$.

Equation (7), with $\eta = \sigma dW$, is a linear stochastic differential equation of a form that is now referred to as a Langevin equation, where $W(t)$ is a normalized Brownian motion or Wiener process. The necessary stochastic concepts are explained at a comfortable level in Dijkstra, (2013, Chapter 3). Einstein’s main results are that

$$\mathcal{E}[u^2] = \frac{\tau^*}{2\lambda}, \quad \mathcal{E}[x^2] = \frac{\tau^*}{\lambda^2} t, \quad (8)$$

with $x(t) = x_0 + \int_0^t u(s) ds$ the displacement of the particle and $\tau^* = \int_{-\infty}^{+\infty} \sigma^2 \delta(s) ds$. There are two remarkable features in equation (8) above. First, the fact that the variance $\mathcal{E}[x^2]$ of the displacement is proportional to time. This leads to the mathematical theory of stochastic differential equations distinguishing between the time differential dt and the stochastic differential dW , since $\int_0^t ds = t$, while $\int_0^t dW(s) = t^2$; in other words, $dW \propto (dt)^{1/2}$.

Second, the friction coefficient λ characterizes in this simple case a dissipation of the fluctuations, since $\mathcal{E}[u(t)] = \mathcal{E}[u_0] \exp(-\lambda t)$. More generally, as Kubo, (1966, section 2) points out, the dissipation constant is $D = \lim_{t \rightarrow \infty} \mathcal{E}[(x(t) - x(0))^2]$, and one gets

$$\mu = \frac{D}{kT} = \frac{1}{kT} \int_0^\infty \mathcal{E}[u(t_0)u(t_0 + t)]dt; \quad (9)$$

here $\mu = 1/\lambda$ is the mobility of the particles, T is the temperature of the thermal bath, and k is the Boltzmann constant. And *voilà*, you have the original and simplest version of FDT, where the acronym also stands for the fluctuation-dissipation theorem.

FDT in general can thus be used either to infer the statistics of thermal fluctuations from the drag law (e.g., Nyquist, 1928) with known λ or the reverse (e.g., Onsager, 1931). The former is more practical in laboratory or industrial situations, like an electric circuit, where it is relatively easy to measure the admittance or impedance of the system and we are not that interested in details of what happens at such-and-such a location in an individual wire. It is the latter, though, that is more useful for natural systems, like the climate system, where we have many observations localized in time and space, and wish to estimate future response to as-yet-unknown forcings.

All of the above apply, however, to systems in thermodynamic equilibrium, and most natural systems—including, of course, the climate system—are not. As Kubo (1966) notes, it is precisely for this reason that FDT has attracted much greater attention “recently”—that is, in the middle of the twentieth century—due to its being extended to “nonequilibrium states [and to] irreversible processes in general.”

FDT applications. At this stage, one should note that nonequilibrium and nonlinearity are, in principle, totally distinct concepts, neither of which implies or includes the other. But, in practice, both of them are often pertinent to the study of complex systems and that is the case for the Earth system as a whole, as well as for its various components.

Thus, for instance, Cecil E. (“Chuck”) Leith (1975) showed that FDT applies to a 2-D or QG turbulent flow with two integral invariants, kinetic energy E and enstrophy Z , under additional assumptions of normal distribution of the realizations and stationarity. Such flows were reviewed in section 4.2 herein. Subject to the above assumptions (Leith, 1975), the unperturbed covariance matrix \mathbf{U} and the average response matrix \mathbf{G} are then related by the FDT relation

$$\mathbf{U}(\tau) = \mathbf{G}(\tau)\mathbf{U}(0), \quad (10)$$

where τ is the interval over which we wish to estimate the response of the system to an arbitrary external forcing. Noting that the regression matrix \mathbf{R} for linear prediction of the stationary multivariate time series with lagged covariance matrix \mathbf{U} equals \mathbf{G} , one then gets that

$$\mathbf{R}(\tau) = \mathbf{U}(\tau)\mathbf{U}^{-1}(0). \quad (11)$$

Since the problem of estimating the response of the climate system to both natural and anthropogenic forcing on multidecadal time scales is becoming scientifically, as well as socioeconomically, more and more important, equations (10) and (11) present a huge advantage over conventional methods of attacking this problem. Indeed, successive assessment reports of the Intergovernmental Panel on Climate Change (IPCC, e.g., IPCC, 2007; Houghton et al., 1990) carried out ensembles of high-end global climate model simulations with a number of prescribed scenarios of such forcings but were limited by the enormous computational expense of such simulations.

In comparison, the linear response of equation (11) can be computed, at least in a reduced subspace of leading eigenvectors of the covariance matrix \mathbf{U} —the so-called empirical orthogonal functions (EOFs; Jolliffe & Cadima, 2016; Preisendorfer, 1988)—relatively easily. And, once that is done, changes in any prescribed scalar or vector observable, say, in the globally averaged surface air temperatures or in the entire sea surface temperature field $\{T_{ij}(t)\}$, can be evaluated in turn for arbitrary small forcings $\delta\mathbf{f}(t)$.

Let $\hat{\mathbf{U}}$ and $\hat{\mathbf{R}}$ be the reduced versions of \mathbf{U} and \mathbf{R} , respectively, with $\{\hat{\mathbf{u}}_\alpha\}$ the EOFs of $\hat{\mathbf{U}}$, and $\{T_\alpha(t)\}$ the projection of said temperature field onto the corresponding EOFs. Component-wise, we can write, following Leith (1975), that

$$\delta T_{\alpha}(t) = \int_{-\infty}^t \sum_{\beta} \hat{R}_{\alpha\beta} \delta f_{\beta}(s) ds. \quad (12)$$

Once more, this is all very helpful for systems in thermodynamic equilibrium and normally distributed stochastic processes, which turbulent fluids and other subsystems of the climate system are not. Given a normal distribution of an initial state, nonlinearity will break that happy state of affairs to a greater or lesser degree.

Generalizations to systems out of equilibrium have been developed since the early 1950s (e.g., Callen & Welton, 1951) and many references appear in Kubo (1966). But a particularly fruitful change in point of view was provided by D. Ruelle, (1998, 2009), who considered the problem in the setting of dynamical systems theory, rather than that of statistical mechanics. The former point of view is justified in this context by the so-called chaotic hypothesis (e.g., Gallavotti & Cohen, 1995), which states, in rough terms, that chaotic systems with many degrees of freedom possess a physically relevant invariant measure ν such that averaging with respect to this measure is equivalent to averaging in time over the system's attractor. This property suffices for using the measure ν in evaluating changes in any observable of the system with respect to any small perturbation, and we return to this point in section 5.3 below.

In the footsteps of Leith (1975), several applications of FDT to climate (e.g., Abramov & Majda, 2008; Gritsun & Branstator, 2007) and ocean (Wirth, 2018) models have been carried out. It is V. Lucarini and colleagues, though, who have systematically applied Ruelle's linear response theory to generalize both equilibrium and transient climate sensitivity (Lucarini et al., 2016; Ragone et al., 2015); they also obtained the resonant response and its spatial patterns in one or more frequency bands for time-dependent forcing (Lucarini et al., 2014, and references therein).

The study of resonant response is made possible by the study of the susceptibility operator $\tilde{\mathbf{S}}$, which is given by the Fourier transform of the linear response operator $\tilde{\mathbf{G}}$. The latter operator requires a generalization of the response matrix \mathbf{G} defined in equation (10) to the nonequilibrium setting, for which we refer to the work of Ruelle, (1998, 2009) and of Lucarini et al. (2014).

5.3. The RDS lamppost

In section 3, we have considered mainly the deterministically nonlinear approach to apprehend the complexities of geosciences in general and climate variability in particular. In the previous subsection, we have also hinted, via the Langevin equation (7), at the complementary approach of stochastically linear dynamics to climate variability and change, due largely to K. Hasselmann (1976). (Imkeller & Von Storch, 2001, and references therein) give a broader view of this approach.

In the present subsection, we briefly outline a promising unification of these two complementary approaches to climate variability and change, via the theory of nonautonomous and of random dynamical systems. This theory is also, as indicated in section 3.2, the proper setting for the study of tipping points, as the open-system generalization of bifurcations (e.g., Ditlevsen & Ashwin, 2018).

The theory of nonautonomous (NDS) and random (RDS) dynamical systems. As a result of sensitive dependence on initial data and on parameters, numerical weather forecasts, as well as climate projections, are both expressed these days in probabilistic terms. It is, in fact, more convenient—and becoming more and more necessary—to rely on a model's (or set of models') probability density function (PDF) rather than on its individual, pointwise simulations or predictions.

We summarize here results on the surprisingly complex statistical structure that characterizes stochastic nonlinear systems. This complex structure does provide meaningful physical information that is not described by the PDF alone; it lives on a random attractor, which extends the concepts of a strange attractor and of the invariant measure that is supported by it, from the deterministic to the stochastic framework. It is this extension that we describe, in the simplest possible terms, forthwith.

On the road to including random effects, one needs to realize first that the climate system, as well as any of its subsystems, is not closed: it exchanges energy, mass and momentum with its surroundings, whether other subsystems or the interplanetary space and the solid earth. Typical applications of dynamical systems theory to climate variability so far have only taken into account exchanges that are constant in time, thus keeping the model—whether governed by ODEs, PDEs, or other differential equations—autonomous; that is, the models had coefficients and forcings that were constant in time.

Succinctly, one can write such a system as

$$\dot{\mathbf{X}} = \mathbf{f}(\mathbf{X}; \boldsymbol{\mu}), \quad (13)$$

where \mathbf{X} now may stand for any climate or other geophysical field, while \mathbf{f} is a smooth function of \mathbf{X} and of the vector of parameters $\boldsymbol{\mu}$ but does not depend explicitly on time. Being autonomous greatly facilitated the analysis of a model's solutions. For instance, two distinct trajectories, $\mathbf{X}_1(t)$ and $\mathbf{X}_2(t)$, of a well-behaved, smooth autonomous system cannot pass through the same point in phase space, which helps describe the system's phase portrait. So does the fact that we only need to consider the behavior of solutions $\mathbf{X}(t)$ as we let time t tend to $+\infty$: the resulting sets of points are—possibly multiple—stationary solutions, periodic solutions, and chaotic sets.

We know only too well, however, that the seasonal cycle plays a key role in climate variability on many time scales, while orbital forcing is crucial on the Quaternary time scales of many millennia, and now anthropogenic forcing is of utmost importance on interdecadal time scales. How can one take into account such time-dependent forcings and analyze the nonautonomous systems written succinctly as

$$\dot{\mathbf{X}} = \mathbf{f}(\mathbf{X}, t; \boldsymbol{\mu}), \quad (14)$$

to which they give rise? In equation (14), the dependence of \mathbf{f} on t may be periodic, $\mathbf{f}(\mathbf{X}, t + P) = \mathbf{f}(\mathbf{X}, t)$, as in various ENSO models, with $P = 12$ months, or monotone, $\mathbf{f}(\mathbf{X}, t + \tau) \geq \mathbf{f}(\mathbf{X}, t)$ for $\tau \geq 0$, as in studying scenarios of anthropogenic climate forcing.

To illustrate the fundamental character of the distinction between (13) and (14), consider the simple scalar version of these two equations:

$$\dot{X} = -\beta X, \quad (15a)$$

$$\dot{X} = -\beta X + \gamma t, \quad (15b)$$

respectively. We assume that both systems are dissipative, that is, $\beta > 0$, and that the forcing is monotone increasing, $\gamma \geq 0$, as would be the case for anthropogenic forcing in the industrial era. Lorenz (1963a) pointed out the key role of dissipativity in giving rise to strange, but attracting solution behavior, while Ghil & Childress, 1987 (1987, section 5.4) emphasized its importance and pervasive character in climate dynamics. Clearly, the only attractor for the solutions of equation (15a), given any initial point $X(0) = X_0$, is the fixed point $X = 0$, attained as $t \rightarrow +\infty$.

For the nonautonomous case of equation (15b), though, this forward-in-time approach yields blowup as $t \rightarrow +\infty$, for any initial point. To make sense of what happens in the case of time-dependent forcing, one introduces instead the pullback approach, in which solutions are allowed to still depend on the time t at which we observe them and also on a time s from which the solution is started, $X(s) = X_0$; presumably $s \ll t$. With this little change of approach, one can easily verify that

$$|X(s, t; X_0) - \mathcal{A}(t)| \rightarrow 0 \quad \text{as } s \rightarrow -\infty, \quad (16)$$

for all t and X_0 , where the pullback attractor (PBA) $\mathcal{A}(t)$ is given explicitly by

$$\mathcal{A}(t) = \frac{\gamma(t - 1/\beta)}{\beta}. \quad (17)$$

We thus obtain, in this pullback sense, the intuitively obvious result that the solutions, if started far enough in the past, all approach the time-dependent attractor set $\mathcal{A}(t)$, which grows linearly in time and thus follows the linear forcing.

For the more complicated case of RDSs, where the random attractor \mathcal{A} depends on the particular realization ω of the driving noise, $\mathcal{A} = \mathcal{A}(t; \omega)$, we refer to Chekroun et al. (2011), Ghil et al. (2008), and Dijkstra, (2013, Chapter 4). The beauty and complexity of the results is illustrated herein by four snapshots at successive times $\{t_1, \dots, t_4\}$ for the Lorenz (1963a) model perturbed by multiplicative noise; see Figure 11. Note that the support of the invariant measure $\nu(t; \omega)$ may change quite abruptly, from time t to time $t + \Delta t$; see the

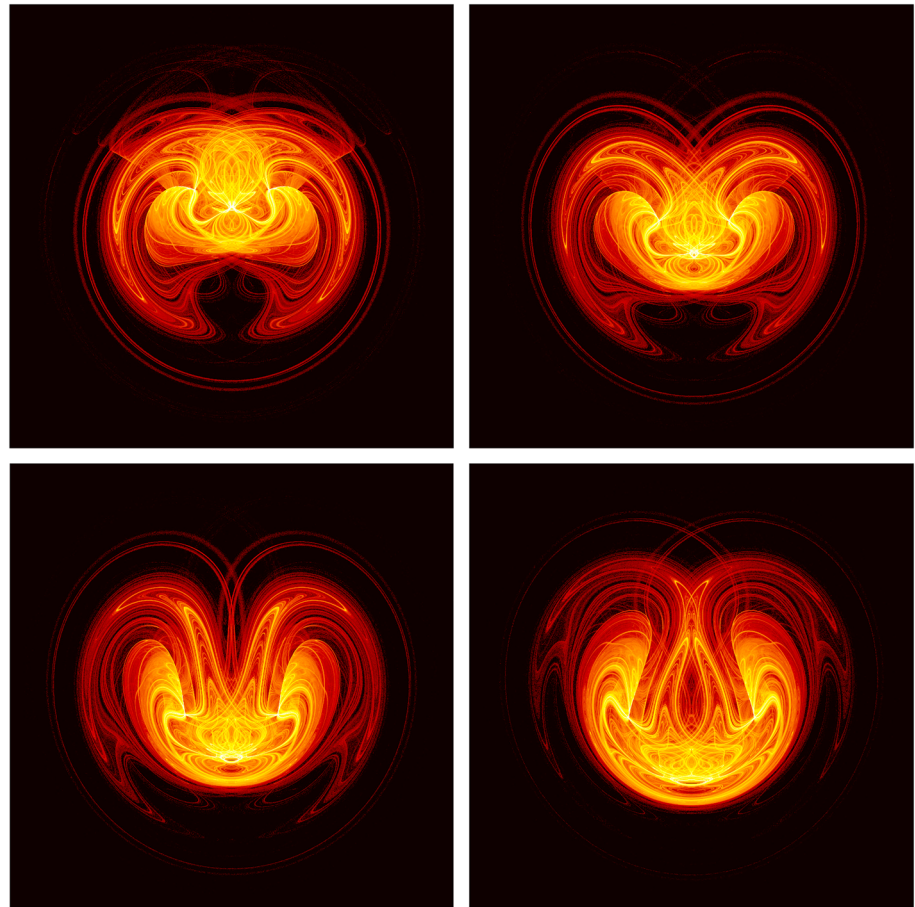


Figure 11. Four snapshots of the stochastically perturbed Lorenz (1963a) model's random attractor $\mathcal{A}(\omega)$ and the invariant measure $\nu(\omega)$ supported on it. The model can be written componentwise as $dX_i = f(\mathbf{X}; \mu)dt + \sigma X_i dW$, $i = 1, 2, 3$, with $\mathbf{X} \equiv (X_1, X_2, X_3) \equiv (X, Y, Z)$ and the parameter values μ equal to the classical ones—normalized Rayleigh number $r = 28$, Prandtl number $Pr = 10$, and normalized wave number $b = 8/3$ —while the noise intensity is $\sigma = 0.5$ and the time step is $\delta t = 5 \cdot 10^{-3}$. The color bar used is on a log-scale and quantifies the probability to end up in a particular region of phase space; shown is a projection of the 3-D phase space (X, Y, Z) onto the (X, Z) plane. Notice the complex, interlaced filament structures between highly (yellow) and moderately (red) populated regions. The time interval Δt between two successive snapshots—moving from left to right and from top to bottom—is $\Delta t = 0.0875$. Weakly populated regions cover an important part of the random attractor and are, in turn, entangled with regions that have near-zero probability (black). (after Chekroun et al., 2011, with permission from Elsevier.)

related short video given as Supplementary Information in Chekroun et al. (2011), as well as at <https://vimeo.com/240039610>. This video shows more clearly than a simple sequence of snapshots the interaction between the nonlinearly deterministic dynamics and the stochastic perturbations.

NDS and RDS applications. We outline here briefly an application of the theory of NDSs to the so-called double-gyre problem of the wind-driven ocean circulation, following Pierini et al. (2016) and Ghil (2017). The large-scale, near-surface flow of the midlatitude oceans is dominated by the presence of a larger, anticyclonic and a smaller, cyclonic gyre. The two gyres share the eastward extension of western boundary currents, such as the Gulf Stream or Kuroshio, and are induced by the shear in the winds that cross the respective ocean basins. Results for this problem in the presence of a surface wind stress that is constant in time were reviewed briefly in section 3.2; see, in particular, Figures 11 and 2 there.

The model domain used by Pierini et al. (2016) is rectangular, like those in section 3.2, and the model equations are based on the equivalent barotropic QG vorticity equation of Simonnet et al. (2005). This PDE is projected here onto four modes that take into account the presence of a western boundary current by including an exponentially decaying factor for the stream function field, as suggested by Jiang et al. (1995). The forcing is deterministic, aperiodic, and dominated by interdecadal variability.

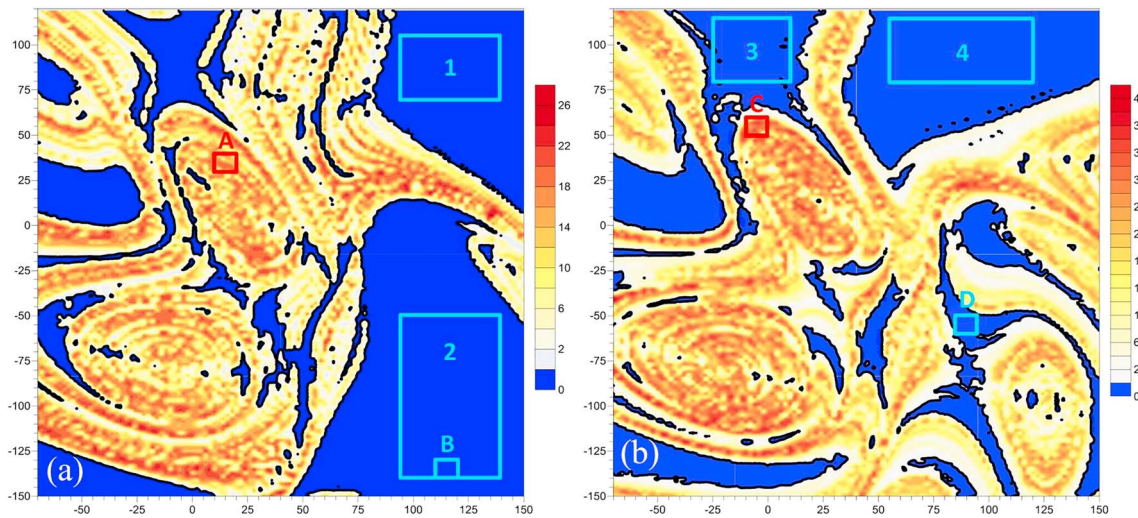


Figure 12. Mean normalized distance Δ for 15,000 trajectories of the double-gyre ocean model: (a) $\gamma = 0.96$, and (b) $\gamma = 1.1$. Reproduced from Pierini et al. (2016). ©American Meteorological Society; used with permission.

The autonomous system exhibits a global bifurcation associated with a homoclinic orbit, like the one illustrated in Figure 2 herein; it occurs at the value $\gamma = 1.0$ for the parameter γ that scales the intensity of the forcing. Pierini et al., 2016 (2016, Appendix) have rigorously demonstrated the existence of a global PBA for the time-dependent forcing case in the weakly dissipative, nonlinear model under discussion, based on general results for nonautonomous dynamical systems (Carvalho et al., 2012; Kloeden & Rasmussen, 2011).

Numerically, though, this unique global attractor seems to possess two separate local PBAs, as apparent from Figure 12. Panels (a) and (b) in the figure refer to parameter values that correspond to subcritical vs. supercritical values of γ in the autonomous model, respectively. While formula 16 seems to require an infinite pullback time, it turns out that convergence to the PBAs in this model only takes about 15 yr.

The mean normalized distance Δ plotted in the figure is defined as $\Delta = \langle \delta_n \rangle_{\bar{T}}$. Here δ_t is the distance, at time t , between two trajectories of the model that were a distance δ_0 apart at time $t = t_0$, and the normalized distance $\delta_n = \delta_t / \delta_0$ is averaged over the whole forward time integration \bar{T} of the available trajectories, with $\bar{T} = 400$ yr.

The maps of Δ in Figure 12 reveal large chaotic regions where $\delta_n \gg 1$ on average (warm colors) and also nonchaotic regions, in which $\sigma \leq 1$ (blue) and thus initially close trajectories do remain close on average. The rectangular regions in the two panels that are labeled by letters A and B and by numbers 1–4 correspond to subdomains of the initial set I (see Pierini et al., 2016, section 5). The numerical evidence in Figure 12 suggests that the boundary between the two types of local attractors has fractal properties.

In the autonomous context, the coexistence of topologically distinct local attractors is well known in the climate sciences (Dijkstra, 2013; Dijkstra & Ghil, 2005; Ghil & Childress, 1987; Simonnet et al., 2005, and references therein). The coexistence of local PBAs with chaotic vs. non-chaotic characteristics, within a unique global PBA, as illustrated by Figure 12 here, seems to be novel, at least in the geosciences literature.

Climate sensitivity and Wasserstein distance. Tamás Tél and associates (Bódai et al., 2011; Bódai & Tél, 2012; Drótos et al., 2015) have applied NDS and RDS concepts and methods to climate modeling, while emphasizing the distinctions and advantages of the pullback point of view with respect to the much more common one of ensemble simulations (IPCC, 2007; Houghton et al., 1990, and references therein). Theoretically speaking, the latter practice merely approximates the PDF that would be obtained by the forward-in-time solution of the Fokker-Planck equation associated with a given model, a solution that is impossible to obtain for high-dimensional climate models (Leith, 1974). An important point raised by the work of these authors is that, aside from the computational difficulties with ensemble size and the PDF approximation, the finite-time averages obtained by the ensemble method do not reflect correctly the changes in time of the climate system's statistics in a transient world.

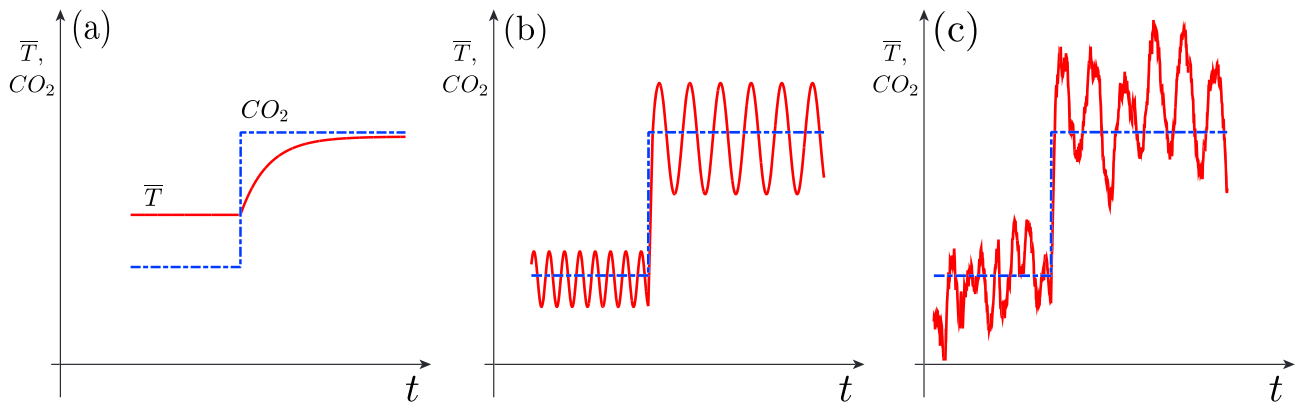


Figure 13. Climate sensitivity (a) for an equilibrium model; (b) for a nonequilibrium, oscillatory model; and (c) for a nonequilibrium, chaotic model, including possibly random perturbations. As a forcing (atmospheric CO₂ concentration, say, dash-dotted line) changes suddenly, global temperature (light solid) undergoes a transition: in panel (a) only the mean temperature changes; in panel (b) the mean adjusts, as it does in panel (a), but the period, amplitude and phase of the oscillation can also decrease, increase or stay the same, while in panel (c) the entire intrinsic variability changes as well. From Ghil (2017), with permission from the American Institute of Mathematical Sciences.

Following up on the work of Lucarini and colleagues (e.g., Lucarini et al., 2014) in applying linear response theory to climate change and on that of Tél and associates above, (Ghil, 2015, 2017) proposed using the Wasserstein or “Earth mover’s” distance Δ_W to generalize the concept of equilibrium climate sensitivity; $\Delta_{W\nu}$ is the distance between two invariant measures of equal mass, ν_1 and ν_2 , on a metric space, like an n -dimensional Euclidean space (Dobrushin, 1970; Kantorovich, 2006; Monge, 1781; Wasserstein, 1969).

Roughly speaking, and dropping the subscript “W,” $\Delta\nu$ represents the total work needed to move the “dirt” (i.e., the measure) from a trench you are digging to another one you are filling, over the distance between the two trenches. One can also view this use of the Wasserstein distance as the truly nonlinear generalization of the FDT approach to climate sensitivity, as reviewed in section 5.2 above.

Equilibrium climate sensitivity γ_e is usually defined as $\gamma_e = \partial\bar{T}/\partial\mu$, where \bar{T} is the globally and seasonally averaged surface air temperature and μ is a parameter, such as the suitably normalized incoming net radiation. It was introduced by Charney et al. (1979) and used extensively by the IPCC’s first three assessment reports (e.g., Houghton et al., 1990). The associated evolution of $\bar{T}(t)$ for a jump in CO₂ concentration in a scalar linear model is illustrated in Figure 13a.

This picture is clearly oversimplified, given the complex evolution of temperatures in the historical record. Figure 13b illustrates $\bar{T}(t)$ in a world in which ENSO would be purely periodic, and Figure 13c illustrates schematically the even more realistic case of temperature evolution in a deterministically chaotic, turbulent and stochastically perturbed system. For such a system, a better definition of climate sensitivity would be

$$\gamma_{cs} = \frac{\Delta\nu}{\Delta\mu}; \quad (18)$$

here $\{\nu_i = \nu_i(\mu_i) : i = 1, 2\}$ can be the invariant measures on a system’s strange attractor, in the autonomous case, or its PBA, whether deterministically nonautonomous or random, and $\{\nu_i = \nu_i(\mu_i) : i = 1, 2\}$ are the corresponding values of a parameter, such as the forcing parameter γ in the Pierini et al. (2016) model in Figure 12. In this sense, one can think of Equation 18 as a generalization of the linear response in Equation (12).

The Wasserstein distance $\Delta(\nu_1, \nu_2)$ between two measures ν_1 and ν_2 on a metric space X is defined as

$$\Delta(\nu_1, \nu_2) = \inf \mathcal{E}[m(\xi, \eta)]; \quad (19)$$

here m is a metric, the infimum is taken over all possible pairs of random variables ξ and η that have the distributions ν_1 and ν_2 , respectively, and \mathcal{E} is the corresponding expectation. When $X = \mathbb{R}$ is just the real line and m the usual Euclidean metric, let Q_1 and Q_2 be the PDFs of the absolutely continuous measures ν_1 and ν_2 . Then

$$\Delta_W(Q_1, Q_2) = \int |G_1(x) - G_2(x)| dx, \quad (20)$$

where G_1 and G_2 are the cumulative distribution functions of the two PDFs Q_1 and Q_2 , respectively (Vallender, 1974).

In general, though, the shape of the two trenches as well as the depth along the trench—that is, both the support of the measure and its density—can differ. Chekroun et al. (2018) have described a so-called critical transition of this type—essentially a generalized tipping point—for a simple ENSO model with a seasonal cycle. In such a case, the actual distance calculations require some model reduction to a smaller phase space (e.g., Kondrashov et al., 2015, and references therein) and they have to rely on more advanced methodologies in the reduced space (e.g., Villani, 2009).

Robin et al. (2017) have argued that the usual quadratic norms used to judge distance in the phase space of climate models do not provide an easy interpretation of the dynamics on the attractor. They calculated the Wasserstein distance between the PBAs of the Lorenz (1984) model subject to summer vs. winter forcings and showed how this metric does provide a more intuitive discrimination between the two.

Vissio and Lucarini (2018) evaluated the performance of a stochastic parametrization by using the Wasserstein distance to measure the difference between the behavior of a full fast-slow system and that of a reduced system in which the parametrization had replaced the fast subsystem. In their setting, the Lorenz (1984) model governed the slow behavior and the Lorenz (1963a) model the fast one. Applying the Wouters and Lucarini (2016) parametrization to the fast component, they showed that “Wasserstein distance provides a robust tool for assessing the quality of the parametrization, and that meaningful results can be obtained when considering [a very coarse-grained] representation of the phase space.”

6. The Way Ahead: Prediction and Prediction

There are two important meanings of “prediction” in the physical sciences. First, there is the relatively straightforward meaning of predicting in time. There are many other areas of science in which one needs, or, at least, wishes to predict: the evolution of an individual illness or of an epidemic, that of human population numbers, the outcomes of national, ethnic, or class conflicts.

In the geosciences, this kind of prediction is clearly of paramount importance: predicting routine weather progress, as well as extreme weather events, like a hurricane landfall or a flash flood, earthquakes, volcanic eruptions, global and regional temperatures, and precipitations many years from now. In all these cases, the usefulness of detailed, physics-based models is largely predicated on the understanding of the phenomena and processes involved. Thus, good predictions validate the knowledge that entered a specific model or class of models, while unsatisfactory ones give a sense of the distance still ahead in the field of interest.

Second, there is the sense in which a theoretical model predicts a phenomenon that had not been observed at the time of the prediction. The paradigmatic example of this kind of prediction is the observational confirmation (Dyson et al., 1920) of the Einstein (1916) prediction of light rays' bending in the gravity field of the Sun. More precisely, the 1919 solar eclipse confirmed that the bending of starlight passing near the Sun was about twice as much as predicted by using Newtonian gravity alone. This kind of prediction tends to be rare, and rather undervalued in the geosciences.

Real-time forecasting. The key difficulty in NWP is the instability and chaotic character of large-scale atmospheric flows. As mentioned in section 4.2, Poincaré (1908) already had the insight that sensitive dependence on initial state will limit the accuracy of weather forecasting. To first order, error growth in the short run is given by the chaotic flows' leading Lyapunov exponent. Over longer times, the flows' mixing properties and scale-invariant cascades contribute to the evolution and saturation of the errors (e.g., Kalnay, 2003 Chapter 6, and references therein).

Since its post World War II beginnings in the mid-1950s, NWP skill has steadily improved over the years; see Thompson (1961) and Kalnay, (2003, Appendix A) for these beginnings. Operational forecasts with good local accuracy in surface air temperatures for up to 3–5 days are fairly routine, although precipitation forecasts, with their greater dependence on more poorly resolved vertical velocities are typically less accurate.

Global forecasts of atmospheric fields on larger scales are much of the time rather accurate up to ten days, thanks to improvements in the physical parametrizations of subgrid-scale phenomena and the assimilation

of massive amounts of remote-sensing data, along with the substantial increase of spatial resolution due to huge increases in computing power and storage capacity.

It appears that the NWP situation is well in hand (e.g., Kalnay, 2003), although there is still room for improvement with respect to the theoretical limits of predictability, of 10–14 days, and substantial misses still occur. Better understanding of the mechanisms associated with the onset, maintenance and termination of blocking, as discussed in section 3.2 herein, could help. And so could a better understanding of the interaction between smaller and larger scales, as reviewed in Palmer and Williams (2009) and in section 4.2 of this review.

John von Neumann's role in starting these modern developments in NWP is well known (cf. Charney et al., 1950). What is a little less so is his longer-range outlook on the three levels of difficulty in understanding and predicting atmospheric and climate phenomena (Von Neumann, 1955): (a) Short-term NWP is the easiest, since it represents a pure initial-value problem, as formulated by Bjerknes (1904) and L. F. Richardson (1922); (b) long-term climate prediction is next easiest, since it corresponds to studying the system's asymptotic behavior, that is, the possible attractors and the statistical properties thereof (Dijkstra & Ghil, 2005; Dijkstra, 2013; Ghil & Childress, 1987); and (c) intermediate-term prediction is hardest, since both the initial data and the parameter values are important.

In fact, long-term climate prediction is a bit harder than Von Neumann envisaged at the time, because the forcing changes in time, too, as discussed here in section 5.3. Concerning the intermediate term, matters tend to get more and more difficult as the prediction horizon is extended further and further, because additional subsystems, with longer time scales and additional evolution mechanisms have to be accounted for (Ghil, 2001).

Thus, subseasonal-to-seasonal prediction is receiving increased attention and is making good progress (Robertson & Vitart, 2018, and references therein). Interannual climate variability being dominated by ENSO, its prediction concentrates on the coupled ocean-atmosphere system in the Tropical Pacific and the teleconnection therefrom to the extratropics. ENSO prediction has made great strides, with the emphasis shifting from statistical and stochastic-dynamic models in the 1990s to high-end climate models in the last decade; compare, for instance, the assessments of real-time ENSO forecast skill in Barnston et al. (1999) vs. Barnston et al. (2012). And interdecadal climate prediction is becoming the hardest problem of the climate sciences, and one of humanity's hardest ones as well.

On the other hand, there are areas of the geosciences in which even the possibility of prediction is viewed with suspicion, for example, earthquake prediction (Geller et al., 1997). In spite of the sustained skepticism, the approach outlined by Zaliapin et al. (2003b) might deserve some attention. A key obstacle to prediction is clearly the relative rarity of large earthquakes and of long and accurate earthquake catalogs. One way to extend the record might be to use a model, albeit a more detailed and complete one than the ternary-tree model mentioned here in section 5.1, to generate additional, synthetic catalogs of arbitrary length, which agree in their statistics with existing catalogs of real sequences, as far as the latter go. And then proceed from there.

The situation with respect to predicting volcanic eruptions is somewhat less controversial than for earthquake prediction but still far from being as routine as in NWP. Some volcanoes, like Mount Etna in Sicily, seem to behave fairly periodically—like the synthetic earthquakes in Figure 10a of section 5.1—and their infrasound rumblings have been used fairly successfully for automated, real-time forecasts (e.g., Hall, 2018). Others behave more irregularly, like in Figure 10b, but still may exhibit characteristic relaxation oscillations of their magma chambers, which could lead to a certain degree of predictability (Walwer et al., 2019).

Predicting new phenomena. The typical way that theory, observation in the field or in the laboratory, and numerical simulation interact in the geosciences is (i) observation in the field, be it the atmosphere, ocean or solid Earth, in situ or remotely; (ii) analysis and description of the observations; and (iii) attempts at explanation of the observed phenomena via competing theories and numerical simulations. Moreover, with increasing computer power and storage capacity, Ockham's razor is neglected more and more, preference being given to high-end models with massive details over the simpler and more easily understandable models.

In fact, philosophical objections do exist to the parsimony principle and it, too, is not infallible. Still, it is simpler to put the Sun at, or near, the center of the solar system than to keep adding epicycles to the

geocentric system (e.g., Kuhn, 1962). The main point of applying the principle is that simpler theories cover more observations and should therefore be easier to falsify, in the terminology of Karl Popper (2005), that is, as the dictionary antonym of “verify” and synonym of “disprove.” Recall that, according to Popper (2005), to be scientific, a statement has to be falsifiable.

A way of using more systematically parsimonious models in the geosciences is that of model hierarchies. Introduced into the climate sciences by Schneider and Dickinson (1974), they extend from simple, low-order conceptual models, through intermediate ones with one or more space dimensions, all the way to high-end ones that encompass many processes and have high 3-D spatial resolution. Rather than hurling epithets of “toy” models toward one end of the hierarchy and “overkill” toward the other, it is important to recognize the role of the entire hierarchy in developing ideas, concepts and tools, on the one hand, and testing them against observations, on the other.

More specifically, Held (2005) has argued for the need to use simpler models in order to understand many aspects of the simulations produced by the more detailed ones. The author of this paper and his colleagues (e.g., Dijkstra & Ghil, 2005; Ghil, 2001; Ghil & Robertson, 2000) have argued that successive bifurcations can play the role of Ariadne’s thread across the rungs of this hierarchy. An illustration of this role in the case of the double-gyre problem for the wind-driven ocean circulation was given in section 3.2.

It is important also to remember that when a simpler model and a more detailed disagree, it is not always the former that is wrong; that is, adding details does not always add realism. Ghil (2015) reviewed a situation of this type, based on the work of Dijkstra (2007). Inspired by the work of Stommel (1961), a series of papers using THC models from simple to intermediate and beyond, had obtained bistability of the meridional-overturning circulation, especially in situations mimicking the Atlantic Ocean; see Dijkstra & Ghil, 2005 (2005, section 3) and Dijkstra, (2005, Chapter 6) for a review.

High-end ocean models used in the third Coupled-Model Intercomparison Program— on which the conclusions of the IPCC’s Fourth Assessment Report (IPCC, 2007) were based — obtained, however, results that contradicted this bistability. As shown by Dijkstra (2007), observations of the evaporation-minus-precipitation fluxes over the Atlantic, between the southern tips of Greenland and Africa, tend to agree better with the simpler models than with the third Coupled-Model Intercomparison Program ones; and it is this better agreement that supports the bistability results of the former, simpler models.

One more interesting story of bistability will shed further light on the correct use of a model hierarchy, as well as on that of nonlinearity in the geosciences in general. EBMs are fairly simple climate models that emphasize the role of incoming and outgoing radiative fluxes in determining the atmosphere’s temperature field, while parameterizing the role of the velocity field in the energy fluxes (Budyko, 1969; Sellers, 1969). Studies of the number and stability of the stationary solutions of these models in the early and mid-1970s showed that—in spite of various differences in their physical formulation and mathematical details (e.g., Ghil & Childress, 1987, Table 10.1)—they exhibited two stable stationary solutions separated in phase space by an unstable one (Ghil, 1976; Held & Suarez, 1974; North et al., 1979).

The warmer of the two stable fixed points could be identified with something like the present climate or, more generally, an interglacial one. The colder one corresponds to an ice-covered planet and was labeled at the time a “deep freeze.” The unstable fixed point (e.g., Bódai et al., 2015) has been explored more recently by using an edge tracking algorithm (Lucarini & Bódai, 2017).

The presence of the saddle-node bifurcation between the interglacial climate and the unstable one was promptly confirmed by the results of a simple general circulation model Wetherald & Manabe, 1975 (1975, Figure 5). In fact, the authors of the latter study commented that “As stated in the Introduction, it is not, however, reasonable to conclude that the present results are more reliable than the results from the one-dimensional studies mentioned above simply because our model treats the effect of transport explicitly rather than by parameterization. [...] Nevertheless, it seems to be significant that both the one-dimensional and three-dimensional models yields qualitatively similar results in many respects.”

In spite of this encouraging confirmation, the fact that a sharp global temperature drop by tens of degrees Celsius could occur given very small insolation changes was not taken seriously for quite a while by many climate scientists. The thinking went that the Sun is a main sequence star and its radiative flux had thus been larger in the past and not smaller, as required by the models for a deep freeze to set in. More recently,

though, considerable evidence has accumulated for Neoproterozoic (1,000–543 Myr ago) glaciations at low latitudes, which suggest a completely glaciated Earth, labeled “snowball Earth” (e.g., Hoffman et al., 1998).

Considerable disagreement persists as to whether the Neoproterozoic glaciation was total or partial, a slushball rather than a snowball; it seems, moreover, to have consisted of ups and downs in temperatures and ice cover, somewhat like the Quaternary glaciation cycles, only longer and stronger. Even so, the much greater difficulty in getting out of a glaciated Earth than into it (e.g., Crowley et al., 2001; Pierrehumbert, 2004) is in substantial agreement with early EBM results on the hysteresis cycle of transition between the high- and low-temperature solution branches (e.g., Ghil, 2001 Figure 1). Finally, atmospheric composition and life clearly played a role not accounted for in the early work on EBMs or Quaternary glaciations (Rothman et al., 2003; Tziperman et al., 2011, and references therein).

To summarize, simple models can offer predictive insights into phenomena only discovered after such a prediction. And nonlinear concepts and methods—applied consistently across a hierarchy of models—can help disentangle the additional complexities to be explained once the phenomena have been identified in observations and described in greater detail.

7. Coda

We have visited several lampposts that have shed a little light—over the last century, and especially its more recent decades—into the darkness of phenomena in the geosciences in general, and into Earth’s fluid envelopes and the climate sciences more specifically. In each case, we have tried to outline the basic ideas and methods that fuel and focus this light, and to give a few examples of successful application of the theoretical ingredients to some of the phenomena. It is time to conclude with the hope that more lampposts will spring up over the coming century and that the overlaps between pairs and triplets of circles of light will provide even greater clarity.

Appendix A : Acronyms

Given the interdisciplinary nature of this review, all acronyms used in the main text are listed in Table A1.

Acronym	Meaning
BDE	Boolean delay equation
CA	cellular automaton (sing.) or automata (pl.)
CN s	complex networks
DDE	delay differential equation
DNS	direct numerical simulation
ER	Erdős-Rényi (network)
FDE	functional differential equation
GFD	geophysical fluid dynamics
IPCC	International Panel on Climate Change
NAO	North Atlantic Oscillation
NDS	nonautonomous dynamical system
MHD	magnetohydrodynamics
OΔE	ordinary difference equation
ODE	ordinary differential equation
P-map	Poincaré map
PΔE	partial difference equation
PDE	partial differential equation
PSA	Pacific-South American (pattern)
QG	quasi-geostrophic (flow, model)
RA	Random acyclic (network)
RDS	Random dynamical system

Acknowledgments

It is a distinct pleasure to express my deepest gratitude to all my graduate students, postdocs, other coauthors, and colleagues, from and with whom I learned most of what I know about the material covered, however imperfectly, in this review paper. I am also grateful to Annick Pouquet, who solicited the paper in the context of this Special Issue and gave me therewith the opportunity to take a view that is both longer and broader than in one's usual research papers. Niklas Boers, Valerio Lucarini, James C. McWilliams, and Annick Pouquet carefully read the draft and provided detailed and very helpful input. Niklas Boers, Shi Jiang, and Fei-Fei Jin kindly provided Figures 5, 1, and 9, respectively; Figures 1 and 9 are based on the numerical results reported in Jiang et al. (1995) and Jin et al. (1994), respectively. An anonymous reviewer provided detailed and constructive input that further improved the paper. This review relies on knowledge accumulated over four decades of support by the European Union's New and Emerging Science and Technology (NEST) Programme; the French Agence Nationale de la Recherche and Centre National de la Recherche Scientifique; and the U.S. Department of Energy, National Air and Space Administration, National Science Foundation, and Office of Naval Research's Multidisciplinary University Research Initiative (MURI).

References

Abramov, R. V., & Majda, A. J. (2008). New approximations and tests of linear fluctuation-response for chaotic nonlinear forced-dissipative dynamical systems. *Journal of Nonlinear Science*, *18*(3), 303–341.

Albert, R., & Barabási, A. L. (2002). Statistical mechanics of complex networks. *Reviews of Modern Physics*, *74*(1), 47–97.

Andronov, A. A., Vitt, A. A., & Khaikin, S. E. (1966). Theory of oscillators. Pergamon Press; republished in 2013 by Elsevier as vol. 4 of their *Adiwes International Series in Physics*.

Arnol'd, V. I. (2012). Geometrical methods in the theory of ordinary differential equations. Springer Science & Business Media; first Russian edition 1978.

Ashwin, P., Wieczorek, S., Vitolo, R., & Cox, P. (2012). Tipping points in open systems: Bifurcation, noise-induced and rate-dependent examples in the climate system. *Philosophical Transactions of the Royal Society A: Mathematical, Physical and Engineering Sciences*, *370*(1962), 1166–1184.

Barenblatt, G. I. (1996). *Scaling, self-similarity, and intermediate asymptotics*. Cambridge, UK: Cambridge University Press.

Barnston, A. G., Glantz, M. H., & He, Y. (1999). Predictive skill of statistical and dynamical climate models in SST forecasts during the 1997–98 El Niño episode and the 1998 La Niña onset. *Bulletin of the American Meteorological Society*, *80*(2), 217–244.

Barnston, A. G., Tippett, M. K., Heures, M. L., Li, S., & DeWitt, D. G. (2012). Skill of real-time seasonal ENSO model predictions during 2002–2011—Is our capability improving? *Bulletin of the American Meteorological Society*, *93*(5), 631–651. <https://doi.org/10.1175/BAMS-D-11-00111.1>

Batchelor, G. K. (1953). *The theory of homogeneous turbulence*. Cambridge, UK: Cambridge University Press.

Baur, F. (1947). *Musterbeispiele Europäischer Grosswetterlagen*. Dietrich: Wiesbaden.

Ben-Zion, Y. (2008). Collective behavior of earthquakes and faults: Continuum-discrete transitions, progressive evolutionary changes, and different dynamic regimes. *Reviews of Geophysics*, *46*, RG4006. <https://doi.org/10.1029/2008RG000260>

Bénard, H. (1900). Les tourbillons cellulaires dans une nappe liquide. *Revue générale de Sciences pures et appliquées*, *11*, 1261–1271.

Benzi, R., & Biferale, L. (2009). Fully developed turbulence and the multifractal conjecture. *Journal of Statistical Physics*, *135*(5), 977–990. <https://doi.org/10.1007/s10955-009-9738-9>

Benzi, R., Malguzzi, P., Speranza, A., & Sutera, A. (1986). The statistical properties of general atmospheric circulation: Observational evidence and a minimal theory of bimodality. *Quarterly Journal of the Royal Meteorological Society*, *112*(473), 661–674. <https://doi.org/10.1002/qj.49711247306>

Bjerknes, V. (1904). Das Problem der Wettervorhersage, betrachtet vom Standpunkte der Mechanik und der Physik. *Meteorologische Zeitschrift*, *21*, 1–7.

Bjerknes, J. (1969). Atmospheric teleconnections from the equatorial Pacific. *Monthly Weather Review*, *97*(3), 163–172.

Bódai, T., Károlyi, G., & Tél, T. (2011). A chaotically driven model climate: Extreme events and snapshot attractors. *Nonlinear Processes in Geophysics*, *18*(5), 573–580. <https://doi.org/10.5194/npg-18-573-2011>

Bódai, T., Lucarini, V., Lunkeit, F., & Boschi, R. (2015). Global instability in the Ghil-Sellers model. *Climate Dynamics*, *44*, 3361–3381.

Bódai, T., & Tél, T. (2012). Annual variability in a conceptual climate model: Snapshot attractors, hysteresis in extreme events, and climate sensitivity. *Chaos: An Interdisciplinary Journal of Nonlinear Science*, *22*(2), 023110. <https://doi.org/10.1063/1.3697984>

Boers, N., Bookhagen, B., Marwan, N., Kurths, J., & Marengo, J. (2013). Complex networks identify spatial patterns of extreme rainfall events of the South American Monsoon System. *Geophysical Research Letters*, *40*, 4386–4392. <https://doi.org/10.1029/2012GL051586>

Boers, N., Goswami, B., Rheinwalt, A., Bookhagen, B., Hoskins, B., & Kurths, J. (2019). Complex networks reveal global pattern of extreme-rainfall teleconnections. *Nature*, *566*, 373–377. <https://doi.org/10.1038/s41586-018-0872-x>

Bradshaw, P., & Huang, G. P. (1995). The law of the wall in turbulent flow. *Proceedings of the Royal Society of London. A*, *451*(1941), 165–188.

Budyko, M. I. (1969). The effect of solar radiation variations on the climate of the Earth. *Tellus*, *21*, 611–619.

Burridge, R., & Knopoff, L. (1967). Model and theoretical seismicity. *Bulletin of the Seismological Society of America*, *57*(3), 341–371.

Busse, F. H. (1978). Non-linear properties of thermal convection. *Reports on Progress in Physics*, *41*, 1929–1967.

Callen, H. B., & Welton, T. A. (1951). Irreversibility and generalized noise. *Physical Review*, *83*(1), 34–40.

Cantor, G. (1887). Mitteilungen zur Lehre vom Transfiniten. *Zeitschrift für Philosophie und philosophische Kritik*, *91*, 81–125.

Cartwright, M. L., & Littlewood, J. E. (1945). On non-linear differential equations of the second order: I. The equation $\ddot{y} - k(1 - y^2)\dot{y} + y = b \cos(\lambda t + \alpha)$, k large. *Journal of the London Mathematical Society*, *1*(3), 180–189.

Carvalho, A., Langa, J. A., & Robinson, J. (2012). *Attractors for infinite-dimensional non-autonomous dynamical systems*. New York, NY: Springer Science & Business Media.

Charney, J. G. (1947). The dynamics of long waves in a baroclinic westerly current. *Journal of Meteorology*, *4*(5), 136–162. [https://doi.org/10.1175/1520-0469\(1947\)004<0136:TDLWI>2.0.CO;2](https://doi.org/10.1175/1520-0469(1947)004<0136:TDLWI>2.0.CO;2)

Charney, J. G. (1971). Geostrophic turbulence. *Journal of the Atmospheric Sciences*, *28*(6), 1087–1095.

Charney, J. G., Arakawa, A., Baker, D. J., Bolin, B., Dickinson, R. E., Goody, R. M., & Wunsch, C. I. (1979). *Carbon dioxide and climate: A scientific assessment*. Washington, DC: National Academy of Sciences.

Charney, J. G., & DeVore, J. G. (1979). Multiple flow equilibria in the atmosphere and blocking. *Journal of the Atmospheric Sciences*, *36*, 1205–1216. [https://doi.org/10.1175/1520-0469\(1979\)036<1205:mfeita>2.0.co;2](https://doi.org/10.1175/1520-0469(1979)036<1205:mfeita>2.0.co;2)

Charney, J. G., Fjørtoft, R., & von Neumann, J. (1950). Numerical integration of the barotropic vorticity equation. *Tellus*, *2*, 237–254.

Charney, J. G., Shukla, J., & Mo, K. C. (1981). Comparison of a barotropic blocking theory with observation. *Journal of the Atmospheric Sciences*, *38*(4), 762–779.

Chekroun, M. D., Ghil, M., & Neelin, J. D. (2018). Pullback attractor crisis in a delay differential ENSO model. In A. A. Tsonis (Ed.), *Advances in Nonlinear Geosciences* (pp. 1–33). New York, NY: Springer Science & Business Media. <https://doi.org/10.1007/978-3-319-58895-7>

Chekroun, M. D., Simonnet, E., & Ghil, M. (2011). Stochastic climate dynamics: Random attractors and time-dependent invariant measures. *Physica D: Nonlinear Phenomena*, *240*(21), 1685–1700. <https://doi.org/10.1016/j.physd.2011.06.005>

Chorin, A. J. (2013). Vorticity and turbulence. Springer Science & Business Media, First published in 1994 vol. 103.

Colon, C., & Ghil, M. (2017). Economic networks: Heterogeneity-induced vulnerability and loss of synchronization. *Chaos*, *27*, 126703.

Coluzzi, B., Ghil, M., Hallegatte, S., & Weisbuch, G. (2011). Boolean delay equations on networks in economics and the geosciences. *International Journal of Bifurcation and Chaos*, *21*(12), 3511–3548. <https://doi.org/10.1142/S0218127411030702>

Constantin, P., Foias, C., Nicolaenko, B., & Temam, R. (1989). *Integral manifolds and inertial manifolds for dissipative partial differential equation*. Berlin-Heidelberg: Springer Science & Business Media.

Cooke, R. (2011). The history of mathematics: A brief course. 2, John Wiley & Sons.

Crowley, T. J., Hyde, W. T., & Peltier, W. R. (2001). CO₂ levels required for deglaciation of a “near-snowball” Earth. *Geophysical Research Letters*, *28*(2), 283–286. <https://doi.org/10.1029/2000gl011836>

- Cushman-Roisin, B., & Beckers, J. M. (2011). Introduction to geophysical fluid dynamics: Physical and numerical aspects. 2, Academic Press.
- Darby, M. S., & Mysak, L. A. (1993). A Boolean delay equation model of an interdecadal Arctic climate cycle. *Climate Dynamics*, 8, 241–246. <https://doi.org/10.1007/BF00198618>
- Dawson, A., & Palmer, T. N. (2014). Simulating weather regimes: Impact of model resolution and stochastic parameterization. *Climate Dynamics*, 44(7-8), 2177–2193. <https://doi.org/10.1007/s00382-014-2238-x>
- Dee, D., & Ghil, M. (1984). Boolean difference equations, I: Formulation and dynamic behavior. *SIAM Journal on Applied Mathematics*, 44(1), 111–126. <https://doi.org/10.1137/0144009>
- Dijkstra, H. A. (2005). *Nonlinear physical oceanography: A dynamical systems approach to the large scale ocean circulation and El Niño* (2nd). Berlin/Heidelberg: Springer Science+Business Media.
- Dijkstra, H. A. (2007). Characterization of the multiple equilibria regime in a global ocean model. *Tellus A: Dynamic Meteorology and Oceanography*, 59(5), 695–705.
- Dijkstra, H. A. (2013). *Nonlinear climate dynamics*. Cambridge, UK: Cambridge University Press.
- Dijkstra, H. A., & Ghil, M. (2005). Low-frequency variability of the large-scale ocean circulation: A dynamical systems approach. *Reviews of Geophysics*, 43, RG3002. <https://doi.org/10.1029/2002RG000122>
- Ditlevsen, P. D., & Ashwin, P. B. (2018). Complex climate response to astronomical forcing: The middle-Pleistocene transition in glacial cycles and changes in frequency locking. *Frontiers in Physics*, 6, 62. <https://doi.org/10.3389/fphy.2018.00062>
- Dobrushin, R. L. (1970). Prescribing a system of random variables by conditional distributions. *Theory of Probability & Its Applications*, 15(3), 458–486.
- Dole, R. M., & Gordon, N. D. (1983). Persistent anomalies of the extratropical Northern Hemisphere wintertime circulation: geographical distribution and regional persistence characteristics. *Monthly Weather Review*, 111(8), 1567–1586. [https://doi.org/10.1175/1520-0493\(1983\)111<1567:paoten>2.0.co;2](https://doi.org/10.1175/1520-0493(1983)111<1567:paoten>2.0.co;2)
- Donges, J. F., Zou, Y., Marwan, N., & Kurths, J. (2009). The backbone of the climate network. *EPL (Europhysics Letters)*, 87(4), 48007.
- Donges, J. F., Zou, Y., Marwan, N., & Kurths, J. (2009). Complex networks in climate dynamics. *The European Physical Journal Special Topics*, 174(1), 157–179.
- Drótos, G., Bódai, T., & Tél, T. (2015). Probabilistic concepts in a changing climate: A snapshot attractor picture. *Journal of Climate*, 28, 3275–3288. <https://doi.org/10.1175/JCLI-D-14-00459.1>
- Dubrulle, B. (2019). Beyond Kolmogorov cascades. *Journal of Fluid Mechanics*, 867, P1. <https://doi.org/10.1017/jfm.2019.98>
- Duffing, G. (1918). *Erzwungene Schwingungen bei veränderlicher Eigenfrequenz und ihre technische Bedeutung*, vol. 41/42. Braunschweig: R. Vieweg & Sohn.
- Dyson, F. A., Eddington, A. S., & Davidson, C. (1920). IX. A determination of the deflection of light by the Sun's gravitational field, from observations made at the total eclipse of May 29, 1919. *Philosophical Transactions of the Royal Society A: Mathematical, Physical and Engineering Sciences*, 220(571–581), 291–333.
- Eady, E. T. (1949). Long waves and cyclone waves. *Tellus*, 1(3), 33–52. <https://doi.org/10.1111/j.2153-3490.1949.tb01265.x>
- Eckmann, J. P. (1981). Roads to turbulence in dissipative dynamical systems. *Reviews of Modern Physics*, 53, 643–654.
- Eckmann, J. P., & Ruelle, D. (1985). Ergodic theory of chaos and strange attractors. *Reviews of Modern Physics*, 57, 617–656.
- Einstein, A. (1905). Über die von der molekularkinetischen Theorie der Wärme geforderte Bewegung von in ruhenden Flüssigkeiten suspendierten Teilchen. *Annalen der Physik*, 322(8), 549–560. reprinted in *Investigations on the Theory of the Brownian Movement*, five articles by A. Einstein, R. Furth (ed.) and A. D. Cowper (transl.), 1956, Dover Publ., New York, 122 pp.
- Einstein, A. (1916). Die Grundlage der allgemeinen Relativitätstheorie (The foundation of the general theory of relativity). *Annalen der Physik*, 354(7), 769–822.
- Farmer, J. D., Ott, E., & Yorke, J. A. (1983). The dimension of chaotic attractors. *Physica D: Nonlinear Phenomena*, 7(1-3), 153–180.
- Fatou, P. (1919). Sur les équations fonctionnelles. *Bulletin de la Société Mathématique de France*, 47, 161–271.
- Fermi, E., Pasta, P., Ulam, S., & Tsingou, M. (1955). *Studies of nonlinear problems, I*. Los Alamos, NM: Los Alamos Scientific Laboratory. <https://doi.org/10.2172/4376203>
- Fjørtoft, R. (1953). On the changes in the spectral distribution of kinetic energy for twodimensional, nondivergent flow. *Tellus*, 5(3), 225–230.
- Frisch, U. (1995). *Turbulence: The legacy of A. N. Kolmogorov*. Cambridge, UK: Cambridge University Press.
- Fujiwara, Y., & Aoyama, H. (2010). Large-scale structure of a nation-wide production network. *The European Physical Journal B*, 77(4), 565–580. <https://doi.org/10.1140/epjb/e2010-00275-2>
- Fultz, D., Long, R. R., Owens, G. V., Bohan, W., Kaylor, R., & Weil, J. (1959). *Studies of thermal convection in a rotating cylinder with some implications for large-scale atmospheric motions, meteorological monographs* (Vol. 4). Boston, Mass: American Meteorological Society.
- Gallavotti, G., & Cohen, E. G. D. (1995). Dynamical ensembles in stationary states. *Journal of Statistical Physics*, 80(5-6), 931–970.
- Geller, R. J., Jackson, D. D., Kagan, Y. Y., & Mulargia, F. (1997). Earthquakes cannot be predicted. *Science*, 275(5306), 1616–1616.
- Ghil, M. (1976). Climate stability for a Sellers-type model. *Journal of the Atmospheric Sciences*, 33(1), 3–20.
- Ghil, M. (2001). Hilbert problems for the geosciences in the 21st century. *Nonlinear Processes in Geophysics*, 8(4/5), 211–211. <https://doi.org/10.5194/npg-8-211-2001>
- Ghil, M. (2015). A mathematical theory of climate sensitivity or, How to deal with both anthropogenic forcing and natural variability? In C. P. Chang, M. Ghil, M. Latif, & J. M. Wallace (Eds.), *Climate change: Multidecadal and beyond* (pp. 31–51): World Scientific Publishing Co./Imperial College Press.
- Ghil, M. (2017). The wind-driven ocean circulation: Applying dynamical systems theory to a climate problem. *Discrete and Continuous Dynamical Systems - A*, 37(1), 189–228. <https://doi.org/10.3934/dcds.2017008>
- Ghil, M., Allen, M. R., Dettinger, M. D., Ide, K., Kondrashov, D., Mann, M. E., & Yiou, P. (2002). Advanced spectral methods for climatic time series. *Reviews of Geophysics*, 40(1), 41. <https://doi.org/10.1029/2000RG000092>
- Ghil, M., Benzi, R., & Parisi, G. (1985). *Turbulence and predictability in geophysical fluid dynamics and climate dynamics*. Amsterdam and New York: North-Holland.
- Ghil, M., Chekroun, M. D., & Simonnet, E. (2008). Climate dynamics and fluid mechanics: Natural variability and related uncertainties. *Physica D: Nonlinear Phenomena*, 237(14–17), 2111–2126. <https://doi.org/10.1016/j.physd.2008.03.036>
- Ghil, M., & Childress, S. (1987). *Topics in geophysical fluid dynamics: Atmospheric dynamics, dynamo theory, and climate dynamics*. Berlin/Heidelberg: Springer Science+Business Media. Reissued in pdf, 2012.
- Ghil, M., Groth, A., Kondrashov, D., & Robertson, A. W. (2018). Extratropical sub-seasonal-to-seasonal oscillations and multiple regimes: The dynamical systems view. In A. W. Robertson, & F. Vitart (Eds.), *The gap between weather and climate forecasting: Sub-seasonal to seasonal prediction* pp. 119–142). Amsterdam, The Netherlands: Elsevier.

- Ghil, M., Kimoto, M., & Neelin, J. D. (1991). Nonlinear dynamics and predictability in the atmospheric sciences. *Reviews of Geophysics*, 29(S1), 46–55.
- Ghil, M., & Mullhaupt, A. (1985). Boolean delay equations, II. Periodic and aperiodic solutions. *Journal of Statistical Physics*, 41(1-2), 125–173. <https://doi.org/10.1007/BF01020607>
- Ghil, M., Read, P. L., & Smith, L. A. (2010). Geophysical flows as dynamical systems: The influence of Hide's experiments. *Astronomy & Geophysics*, 51(4), 4.28–4.35.
- Ghil, M., & Robertson, A. W. (2000). Solving problems with GCMs: General circulation models and their role in the climate modeling hierarchy. In D. Randall (Ed.), *General circulation model development: Past, present and future* (pp. 285–325). San Diego: Academic Press.
- Ghil, M., Zaliapin, I., & Coluzzi, B. (2008). Boolean delay equations: A simple way of looking at complex systems. *Physica D: Nonlinear Phenomena*, 237(23), 2967–2986.
- Gill, A. E. (1982). *Atmosphere-ocean dynamics*. New York, U.S.A.: Academic Press.
- Gladwell, M. (2000). *The tipping point: How little things can make a big difference*. Little Brown.
- Gleick, P. (1987). *Chaos: Making a new science*. New York, NY: Penguin Random House.
- Goldstein, S. (1969). Fluid mechanics in the first half of this century. *Annual Review of Fluid Mechanics*, 1(1), 1–29.
- Gozolchiani, A., Havlin, S., & Yamasaki, K. (2011). Emergence of El Niño as an autonomous component in the climate network. *Physical Review Letters*, 107(14), 148501.
- Grassberger, P. (1983). Generalized dimensions of strange attractors. *Physics Letters A*, 97, 227–230.
- Gritsun, A., & Branstator, G. (2007). Climate response using a three-dimensional operator based on the fluctuation–dissipation theorem. *Journal of the Atmospheric Sciences*, 64(7), 2558–2575.
- Groth, A., Feliks, Y., Kondrashov, D., & Ghil, M. (2017). Interannual variability in the North Atlantic ocean's temperature field and its association with the wind stress forcing. *Journal Climate*, 30(7), 2655–2678. <https://doi.org/10.1175/jcli-d-16-0370.1>
- Guckenheimer, J., & Holmes, P. J. (1983). *Nonlinear oscillations, dynamical systems, and bifurcations of vector fields*. New York, NY: Springer Science & Business Media.
- Hadamard, J. (1898). Les surfaces à courbures opposées et leurs lignes géodésique. *Journal des Mathématiques Pures & Appliquées*, 4, 27–73.
- Hall, S. (2018). World's first automated volcano forecast predicts Mount Etna's eruptions: system tracks infrasound waves to determine when an eruption is imminent and alerts the Italian government. *Nature*, 563(7732), 456–457. <https://doi.org/10.1038/d41586-018-07420-y>
- Haller, G. (2015). Lagrangian coherent structures. *Annual Review of Fluid Mechanics*, 47, 137–162.
- Hasselmann, K. (1976). Stochastic climate models. I: Theory. *Tellus*, 28, 473–485.
- Hausdorff, F. (1918). Dimension und äußeres Maß. *Mathematische Annalen*, 79(1-2), 157–179.
- Held, I. M. (2005). The gap between simulation and understanding in climate modeling. *Bulletin of the American Meteorological Society*, 86, 1609–1614. <https://doi.org/10.1175/bams-86-11-1609>
- Held, I. M., & Suarez, M. J. (1974). Simple albedo feedback models of the ice caps. *Tellus*, 26, 613–629.
- Hide, R. (1989). A review of: Topics in geophysical fluid dynamics: Atmospheric dynamics, dynamo theory and climate dynamics. *Geophysical and Astrophysical Fluid Dynamics*, 46(4), 261–270. <https://doi.org/10.1080/03091928908208915>
- Hide, R., & Mason, P. J. (1975). Sloping convection in a rotating fluid. *Advances in Physics*, 24, 45–100.
- Hildebrandsson, H. H., & Teisserenc de Bort, L. P. (1898). *Les bases de la météorologie dynamique: Historique - état de nos connaissances* (Vol. 1). Paris: Gauthier-Villars et Fils.
- Hoffman, P. F., Kaufman, A. J., Halverson, G. P., & Schrag, D. P. (1998). A Neoproterozoic snowball earth. *Science*, 281(5381), 1342–1346.
- Hopf, E. (1948). A mathematical example displaying features of turbulence. *Communications on Pure and Applied Mathematics*, 1(4), 303–322.
- Hoskins, B. J., & Karoly, D. J. (1981). The steady linear response of a spherical atmosphere to thermal and orographic forcing. *Journal of the Atmospheric Sciences*, 38(6), 1179–1196.
- Houghton, J. T., Jenkins, G. J., & Ephraums, J. J. (1990). Climate change: The IPCC scientific assessment. Report Prepared for Intergovernmental Panel on Climate Change by Working Group I, Cambridge, UK, 365+xxxx pp.
- Hunt, J. C. R. (1998). Lewis Fry Richardson and his contributions to mathematics, meteorology, and models of conflict. *Annual Review of Fluid Mechanics*, 30(1), xiii–xxxvi. <https://doi.org/10.1146/annurev.fluid.30.1.0>
- IPCC (2007). *Climate change 2007—The physical science basis: Working Group I Contribution to the Fourth Assessment Report of the IPCC* Edited by (Solomon et al. Ed.) Cambridge, UK and New York, NY, USA: Cambridge University Press. <http://www.worldcat.org/isbn/0521880092>
- Imkeller, P., & Von Storch, J. S. (2001). *Stochastic climate models*. New York, NY: Springer Science & Business Media.
- Isaacson, E., & Keller, H. B. (2012). *Analysis of numerical methods*. Courier Corporation, First published by John Wiley & Sons in 1966; reprinted as a Dover Classic in 1994.
- Jiang, S., Jin, F. F., & Ghil, M. (1995). Multiple equilibria and aperiodic solutions in a wind-driven double-gyre, shallow-water model. *Journal of Physical Oceanography*, 25, 764–786.
- Jin, F. F., & Ghil, M. (1990). Intraseasonal oscillations in the extratropics: Hopf Bifurcation and topographic instabilities. *Journal of the Atmospheric Sciences*, 47(24), 3007–3022. [https://doi.org/10.1175/1520-0469\(1990\)047<3007:ioiteh>2.0.co;2](https://doi.org/10.1175/1520-0469(1990)047<3007:ioiteh>2.0.co;2)
- Jin, F. F., Neelin, J. D., & Ghil, M. (1994). El Niño on the devil's staircase: Annual subharmonic steps to chaos. *Science*, 264, 70–72.
- Jin, F. F., Neelin, J. D., & Ghil, M. (1996). El Niño/Southern Oscillation and the annual cycle: Subharmonic frequency-locking and aperiodicity. *Physica D: Nonlinear Phenomena*, 98, 442–465.
- Jolliffe, I. T., & Cadima, J. (2016). Principal component analysis: A review and recent developments. *Philosophical Transactions of the Royal Society A: Mathematical, Physical and Engineering Sciences*, 374(2065), 20150202.
- Jordan, D. W., & Smith, P. (2007). *Nonlinear ordinary differential equations—An introduction for scientists and engineers* (2nd ed.). Oxford/New York: Oxford University Press.
- Julia, G. (1918). Mémoire sur l'itération des applications fonctionnelles. *Journal des Mathématiques Pures & Appliquées*, 7, 47–245.
- Kalnay, E. (2003). *Atmospheric modeling, data assimilation and predictability*. Cambridge, UK: Cambridge University Press.
- Kantorovich, L. V. (2006). On the translocation of masses. *Journal of Mathematical Sciences*, 133(4), 1381–1382.
- Kaplan, J. L., & Yorke, J. A. (1979). Chaotic behavior of multidimensional difference equations, *Functional differential equations and approximation of fixed points* pp. 204–227). New York, NY: Springer Science & Business Media.
- Kloeden, P. E., & Rasmussen, M. (2011). *Nonautonomous dynamical systems*. Providence, RI: American Mathematical Society.
- Kolmogorov, A. N. (1941). The local structure of turbulence in incompressible viscous fluid for very large Reynolds numbers. *Doklady Akademii Nauk SSSR*, 30, 299–303.

- Kondrashov, D., Chekroun, M. D., & Ghil, M. (2015). Data-driven non-Markovian closure models. *Physica D: Nonlinear Phenomena*, 297, 33–55. <https://doi.org/10.1016/j.physd.2014.12.005>
- Kraichnan, R. H. (1967). Inertial ranges in two-dimensional turbulence. *The Physics of Fluids*, 10(7), 1417–1423.
- Krishnamurthy, V. (2019). Predictability of weather and climate. *Earth and Space Sciences*, 6. <https://doi.org/10.1029/2019EA000586>
- Krishnamurti, R. (1973). Some further studies on the transition to turbulent convection. *Journal of Fluid Mechanics*, 60, 285–303.
- Kubo, R. (1966). The fluctuation-dissipation theorem. *Reports on Progress in Physics*, 29(1), 255–284.
- Kuhn, T. S. (1962). *The structure of scientific revolutions*. Chicago: University of Chicago Press.
- Lamb, H. (1932). *Hydrodynamics*. Cambridge University Press, Reprinted by Dover in 1945 as a "Dover Classic".
- Landau, L. D., & Lifshitz, E. M. (1959). *Fluid mechanics*. Oxford, UK: Pergamon Press.
- Legras, B., & Ghil, M. (1985). Persistent anomalies, blocking, and variations in atmospheric predictability. *Journal of the Atmospheric Sciences*, 42, 433–471.
- Legras, B., Santangelo, P., & Benzi, R. (1988). High-resolution numerical experiments for forced two-dimensional turbulence. *Europhysics Letters*, 5(1), 37–42. <https://doi.org/10.1209/0295-5075/5/1/007>
- Leith, C. E. (1974). Theoretical skill of Monte Carlo forecasts. *Monthly Weather Review*, 102(6), 409–418.
- Leith, C. E. (1975). Climate response and fluctuation dissipation. *Journal of the Atmospheric Sciences*, 32(10), 2022–2026.
- Lenton, T. M., Held, H., Kriegler, E., Hall, J. W., Lucht, W., Rahmstorf, S., & Schellnhuber, H. J. (2008). Tipping elements in the Earth's climate system. *Proceedings of the National Academy of Sciences*, 105, 1786–1793.
- Leonov, G., Kuznetsov, N., Korzhemanova, N., & Kusakin, D. (2016). Lyapunov dimension formula for the global attractor of the Lorenz system. *Communications in Nonlinear Science and Numerical Simulation*, 41, 84–103. <https://doi.org/10.1016/j.cnsns.2016.04.032>
- Li, T. Y., & Yorke, J. A. (1975). Period three implies chaos. *The American Mathematical Monthly*, 82(10), 985–992.
- Libchaber, A. (1985). The onset of weak turbulence. An experimental introduction. In M. Ghil, R. Benzi, & G. Parisi (Eds.), *Turbulence and predictability in geophysical fluid dynamics and climate dynamics* pp. 17–28. Amsterdam & New York: North-Holland.
- Lorenz, E. N. (1963a). Deterministic nonperiodic flow. *Journal of the Atmospheric Sciences*, 20, 130–141.
- Lorenz, E. N. (1963b). The mechanics of vacillation. *Journal of the Atmospheric Sciences*, 20, 448–464.
- Lorenz, E. N. (1984). Irregularity: A fundamental property of the atmosphere. *Tellus A*, 36(2), 98–110.
- Losa, G. A., Ristanović, D., Ristanović, D., Zaletel, I., & Beltraminelli, S. (2016). From fractal geometry to fractal analysis. *Applied Mathematics*, 7, 346–354. <https://doi.org/10.4236/am.2016.74032>
- Lucarini, V., & Bódai, T. (2017). Edge states in the climate system: Exploring global instabilities and critical transitions. *Nonlinearity*, 30(7), R32–R66. <https://doi.org/10.1088/1361-6544/aa6b11>
- Lucarini, V., Blender, R., Herbert, C., Ragone, F., Pascale, S., & Wouters, J. (2014). Mathematical and physical ideas for climate science. *Reviews of Geophysics*, 52, 809–859. <https://doi.org/10.1002/2013RG000446>
- Lucarini, V., Ragone, F., & Lunkeit, F. (2016). Predicting climate change using response theory: Global averages and spatial patterns. *Journal of Statistical Physics*, 166(3–4), 1036–1064. <https://doi.org/10.1007/s10955-016-1506-z>
- Malamud, B. D., Morein, G., & Turcotte, D. L. (1998). Forest fires: An example of self-organized critical behavior. *Science*, 281(5384), 1840–1842.
- Manabe, S., Smagorinsky, J., Holloway, J. L., & Stone, H. M. (1970). Simulated climatology of a general circulation model with a hydrologic cycle. *Monthly Weather Review*, 98(3), 175–212.
- Mandelbrot, B. (1967). How long is the coast of Britain? Statistical self-similarity and fractional dimension. *Science*, 156(3775), 636–638. <https://doi.org/10.1126/science.156.3775.636>
- Mandelbrot, B. (1969). *On intermittent free turbulence. Turbulence of fluids and plasmas*. New York: Wiley - Interscience.
- Mandelbrot, B. (1977). *Fractals*. Freeman San Francisco.
- Mandelbrot, B. (2013). *Fractals and chaos: The Mandelbrot set and beyond*. New York, NY: Springer Science & Business Media.
- Mathieu, J., & Scott, J. (2000). *An introduction to turbulent flow*. Cambridge, UK: Cambridge University Press.
- McLaughlin, J. B., & Martin, P. C. (1975). Transition to turbulence in a statically stressed fluid system. *Physical Review A*, 12(1), 186–203.
- McWilliams, J. C. (1984). The emergence of isolated coherent vortices in turbulent flow. *Journal of Fluid Mechanics*, 146, 21–43. <https://doi.org/10.1017/s00222112084001750>
- McWilliams, J. C. (2011). *Fundamentals of geophysical fluid dynamics* (2nd). Cambridge, UK: Cambridge University Press.
- McWilliams, J. C. (2019). A perspective on the legacy of Edward Lorenz. *Earth and Space Sciences*, 6, 336–350. <https://doi.org/10.1029/2018ea000434>
- Mo, K. C., & Ghil, M. (1987). Statistics and dynamics of persistent anomalies. *Journal of the Atmospheric Sciences*, 44(5), 877–902.
- Monge, G. (1781). Mémoire sur la théorie des déblais et des remblais. *Histoire de l'Académie Royale des Sciences de Paris*, 1781, 666–704.
- Mullhaupt, A. P. (1984). *Boolean delay equations: A class of semidiscrete dynamical systems* (pp. 386). New York, NY: New York University.
- Namias, J. (1950). The index cycle and its role in the general circulation. *Journal of Meteorology*, 7, 130–139.
- Namias, J. (1968). Long-range weather forecasting: History, current status and outlook. *Bulletin of the American Meteorological Society*, 49, 438–470.
- Nastrom, G. D., & Gage, K. S. (1985). A climatology of atmospheric wavenumber spectra of wind and temperature observed by commercial aircraft. *Journal of the Atmospheric Sciences*, 42(9), 950–960.
- Newman, M. E. J. (2010). *Networks: An introduction*. Oxford, UK: Oxford University Press.
- Nicolis, C., & Nicolis, G. (1984). Is there a climatic attractor? *Nature*, 311, 529–532.
- North, G. R., Howard, L., Pollard, D., & Wielicki, B. (1979). Variational formulation of Budyko-Sellers climate models. *Journal of the Atmospheric Sciences*, 36, 255–259.
- Nyquist, H. (1928). Thermal agitation of electric charge in conductors. *Physical Review*, 32(1), 110–113.
- Onsager, L. (1931). Reciprocal relations in irreversible processes. I. *Physical Review*, 37(4), 405–426.
- Onsager, L. (1944). Crystal statistics. I. A two-dimensional model with an order-disorder transition. *Physical Review*, 65(3–4), 117.
- Onsager, L. (1949). Statistical hydrodynamics. *Il Nuovo Cimento (1943-1954)*, 6(2), 279–287.
- Palmer, T. N., & Williams, P. (2009). *Stochastic physics and climate modelling*. Cambridge, UK: Cambridge University Press.
- Pedlosky, J. (1987). *Geophysical fluid dynamics* (2nd). Berlin/Heidelberg: Springer Science & Business Media.
- Peitgen, H. O., & Richter, P. H. (2013). *The beauty of fractals: Images of complex dynamical systems*. New York, NY: Springer Science & Business Media.
- Pierini, S., Chekroun, M. D., & Ghil, M. (2018). The onset of chaos in nonautonomous dissipative dynamical systems: A low-order ocean-model case study. *Nonlinear Processes in Geophysics*, 25, 671–692. <https://doi.org/10.5194/npg-25-671-2018>
- Pierini, S., Ghil, M., & Chekroun, M. D. (2016). Exploring the pullback attractors of a low-order quasigeostrophic ocean model: The deterministic case. *Journal of Climate*, 29(11), 4185–4202.

- Pierrehumbert, R. T. (2004). High levels of atmospheric carbon dioxide necessary for the termination of global glaciation. *Nature*, 429(6992), 646–649. <https://doi.org/10.1038/nature02640>
- Poincaré, H. (1908). *Science et Méthode*. Paris: Ernest Flammarion.
- Popper, K. (2005). The logic of scientific discovery. Routledge, Original German: Logik der Forschung. Zur Erkenntnistheorie der modernen Naturwissenschaft, 1935; first English edition 1959.
- Pouquet, A., Marino, R., Mininni, P. D., & Rosenberg, D. (2017). Dual constant-flux energy cascades to both large scales and small scales. *Physics of Fluids*, 29(11), 111108. <https://doi.org/10.1063/1.5000730>
- Pouquet, A., Stawarz, J. E., Rosenberg, D., & Marino, R. (2019). Helicity dynamics, inverse and bi-directional cascades in fluid and magnetohydrodynamic turbulence: A brief review. *Earth and Space Sciences*, 6, 351–369. <https://doi.org/10.1029/2018ea000432>
- Preisendorfer, R. W. (1988). *Principal component analysis in meteorology and oceanography*. Amsterdam, The Netherlands: Elsevier.
- Press, F., & Allen, C. (1995). Patterns of seismic release in the southern California region. *Journal of Geophysical Research*, 100(B4), 6421–6430.
- Ragone, F., Lucarini, V., & Lunkeit, F. (2015). A new framework for climate sensitivity and prediction: A modelling perspective. *Climate Dynamics*, 46(5-6), 1459–1471. <https://doi.org/10.1007/s00382-015-2657-3>
- Ravelet, F., Chiffaudel, A., & Daviaud, F. (2008). Supercritical transition to turbulence in an inertially driven von Kármán closed flow. *Journal of Fluid Mechanics*, 601, 339–364.
- Rayleigh, J. W. S. (1916). LIX. On the convective currents in a horizontal layer of fluid when the higher temperature is on the under side. *The London, Edinburgh, and Dublin Philosophical Magazine and Journal of Science*, 32, 529–546. <https://doi.org/10.1080/14786441608635602>
- Rhines, P. B. (1979). Geostrophic turbulence. *Annual Review of Fluid Mechanics*, 11(1), 401–441.
- Richardson, L. F. (1922). *Weather prediction by numerical process*. Cambridge, UK: Cambridge University Press.
- Richardson, L. F. (1961). The problem of contiguity: An appendix to statistics of deadly quarrels. *General System Yearbook*, 6, 139–187.
- Robertson, A. W., & Vitart, F. (2018). *The gap between weather and climate forecasting: Sub-seasonal to seasonal prediction*. Amsterdam, Netherlands: Elsevier.
- Robin, Y., Yiou, P., & Naveau, P. (2017). Detecting changes in forced climate attractors with Wasserstein distance. *Nonlinear Processes in Geophysics*, 24(3), 393–405.
- Romanowicz, B. (1993). Spatiotemporal patterns in the energy release of great earthquakes. *Science*, 260(5116), 1923–1926.
- Rothman, D. H., Hayes, J. M., & Summons, R. E. (2003). Dynamics of the Neoproterozoic carbon cycle. *Proceedings of the National Academy of Sciences*, 100(14), 8124–8129. <https://doi.org/10.1073/pnas.0832439100>
- Ruelle, D. (1990). Deterministic chaos: The science and the fiction. *Proceedings of the Royal Society of London*, 427A, 241–248.
- Ruelle, D. (1995). Turbulence, strange attractors, and chaos. vol. 16 World Scientific.
- Ruelle, D. (1998). Nonequilibrium statistical mechanics near equilibrium: Computing higher-order terms. *Nonlinearity*, 11(1), 5–18.
- Ruelle, D. (2009). A review of linear response theory for general differentiable dynamical systems. *Nonlinearity*, 22, 855–870.
- Ruelle, D., & Takens, F. (1971a). On the nature of turbulence. *Communications in Mathematical Physics*, 20, 167–192.
- Ruelle, D., & Takens, F. (1971b). Note concerning our paper “On the nature of turbulence”. *Communications in Mathematical Physics*, 23, 343–344.
- Sagan, H. (2012). *Space-filling curves*. New York, NY: Springer Science & Business Media.
- Sakuma, H., & Ghil, M. (1991). Stability of propagating modons for small-amplitude perturbations. *Physics of Fluids A: Fluid Dynamics*, 3(3), 408–414.
- Salmon, R. (1998). *Lectures on geophysical fluid dynamics*. Oxford, UK: Oxford University Press.
- Saltzman, B. (1962). Finite amplitude free convection as an initial value problem—I. *Journal of the Atmospheric Sciences*, 19, 329–341.
- Saunders, A., & Ghil, M. (2001). A Boolean delay equation model of ENSO variability. *Physica D: Nonlinear Phenomena*, 160(1-2), 54–78.
- Schiesser, W. E. (2012). *The numerical method of lines: Integration of partial differential equations*. Amsterdam, Netherlands: Elsevier.
- Schlichting, H., & Gersten, K. (2016). *Boundary-layer theory* (9th English). New York, NY: Springer Science & Business Media.
- Schneider, S. H., & Dickinson, R. E. (1974). Climate modelling. *Reviews of Geophysics and Space Physics*, 25, 447–493.
- Sellers, W. D. (1969). A global climatic model based on the energy balance of the Earth atmosphere. *Journal of Applied Meteorology*, 8, 392–400.
- Sierpiński, W. (1916). Sur une courbe cantorienne qui contient une image biunivoque et continue de toute courbe donnée. *Comptes Rendus de l'Académie des Sciences de Paris*, 162, 629–632.
- Simonet, E., Ghil, M., & Dijkstra, H. A. (2005). Homocline bifurcations in the quasi-geostrophic double-gyre circulation. *Journal of Marine Research*, 63, 931–956.
- Smale, S. (1967). Differentiable dynamical systems. *Bulletin of the American Mathematical Society*, 73(6), 747–817.
- Smith, L. A. (1988). Intrinsic limits on dimension calculations. *Physics Letters A*, 113, 283–288.
- Sparrow, C. (1982). *The Lorenz equations: Bifurcations, chaos, and strange attractors*. New York, NY: Springer Science & Business Media.
- Spyratos, V., Bourgeron, P. S., & Ghil, M. (2007). Development at the wildland–urban interface and the mitigation of forest-fire risk. *Proceedings of the National Academy of Sciences*, 104(36), 14,272–14,276.
- Steinhaus, H. (1954). Length, shape and area. *Colloquium Mathematicae*, 3, 1–13.
- Stommel, H. (1961). Thermohaline convection with two stable regimes of flow. *Tellus*, 2, 244–230.
- Suppes, P. (1972). *Axiomatic set theory*. Dover.
- Swinney, H. L. (1978). Hydrodynamic instabilities and the transition to turbulence. *Progress of Theoretical Physics Supplement*, 64, 164–175. <https://doi.org/10.1143/PTPS.64.164>
- Takens, F. (1981). Detecting strange attractors in turbulence. In D. A. Rand, & L.-S. Young (Eds.), *Dynamical systems and turbulence, Warwick 1980* (Vol. 898, pp. 366–381). New York, NY: Springer Science & Business Media.
- Temam, R. (2000). *Infinite-dimensional dynamical systems in mechanics and physics* (2nd). New York: Springer Science & Business Media.
- Temam, R. (2001). *Navier-Stokes equations: Theory and numerical analysis*. Providence, RI: American Mathematical Society.
- Thompson, P. D. (1961). *Numerical weather analysis and prediction*. Macmillan.
- Thomson, J. (1882). On a changing tessellated structure in certain liquids. *Proceedings of the Philosophical Society of Glasgow*, 13, 464–468.
- Timoshenko, S. P., & Gere, J. M. (1961). *Theory of elastic stability*. New York, NY: McGraw-Hill.
- Tsonis, A. A., & Elsner, J. B. (1988). The weather attractor over very short timescales. *Nature*, 333, 545–547. <https://doi.org/10.1038/333545a0>
- Tsonis, A. A., & Swanson, K. L. (2008). Topology and predictability of El Niño and La Niña networks. *Physical Review Letters*, 100(22), 228,502–228,506.
- Tsonis, A. A., Swanson, K., & Kravtsov, S. (2007). A new dynamical mechanism for major climate shifts. *Geophysical Research Letters*, 34, L13705. <https://doi.org/10.1029/2007GL030288>

- Tziperman, E., Halevy, I., Johnston, D. T., Knoll, A. H., & Schrag, D. P. (2011). Biologically induced initiation of Neoproterozoic snowball-Earth events. *Proceedings of the National Academy of Sciences*, *108*(37), 15,091–15,096. <https://doi.org/10.1073/pnas.1016361108>
- Vallender, S. S. (1974). Calculation of the Wasserstein distance between probability distributions on the line. *Theory of Probability and its Applications*, *18*(4), 784–786.
- Van der Pol, B. (1920). A theory of the amplitude of free and forced triode vibrations. *Radio Review*, *1*, 701–710.
- Van der Pol, B. (1926). On relaxation-oscillations. *The London, Edinburgh and Dublin Philosophical Magazine and Journal of Science*, *2*, 978–992.
- Veronis, G. (1963). An analysis of the wind-driven ocean circulation with a limited number of Fourier components. *Journal of the Atmospheric Sciences*, *20*, 577–593.
- Villani, C. (2009). *Optimal transport: Old and new*. New York, NY: Springer Science & Business Media.
- Vissio, G., & Lucarini, V. (2018). Evaluating a stochastic parametrization for a fast-slow system using the Wasserstein distance. *Nonlinear Processes in Geophysics*, *25*(2), 413–427. <https://doi.org/10.5194/npg-25-413-2018>
- Von Neumann, J. (1951). The general and logical theory of automata. In L. A. Jeffress (Ed.), *Cerebral mechanisms in behavior; The Hixon symposium* (pp. 1–31). New York, NY: John Wiley & Sons.
- Von Neumann, J. (1955). Some remarks on the problem of forecasting climatic fluctuations. In R. L. Pfeffer (Ed.), *Dynamics of climate* (pp. 9–11). Oxford, UK: Pergamon Press. <https://doi.org/10.1016/b978-1-4831-9890-3.50009-8>
- Walker, G. T., & Bliss, E. W. (1932). World weather V. *Memoirs of the Royal Meteorological Society*, *4*(36), 53–84.
- Wallace, J. M., & Gutzler, D. S. (1981). Teleconnections in the geopotential height field during the Northern Hemisphere winter. *Monthly Weather Review*, *109*, 784–812.
- Walwer, D., Ghil, M., & Calais, E. (2019). Oscillatory nature of the Okmok volcano's deformation. *Earth and Planetary Science Letters*, *506*, 76–86.
- Wasserstein, L. N. (1969). Markov processes over denumerable products of spaces describing large systems of automata. *Problems of Information Transmission*, *5*(3), 47–52.
- Weeks, E. R., Tian, Y., Urbach, J. S., Ide, K., Swinney, H. L., & Ghil, M. (1997). Transitions between blocked and zonal flows in a rotating annulus with topography. *Science*, *278*, 1598–1601.
- Wetherald, R. T., & Manabe, S. (1975). The effects of changing the solar constant on the climate of a general circulation model. *Journal of the Atmospheric Sciences*, *32*(11), 2044–2059.
- Wiin-Nielsen, A. (1967). On the annual variation and spectral distribution of atmospheric energy. *Tellus*, *19*(4), 540–559.
- Wirth, A. (2018). A fluctuation-dissipation relation for the ocean subject to turbulent atmospheric forcing. *Journal of Physical Oceanography*, *48*(4), 831–843.
- Wolfram, S. (1983). Statistical mechanics of cellular automata. *Reviews of Modern Physics*, *55*(3), 601–644.
- Wouters, J., & Lucarini, V. (2016). Parametrization of cross-scale interaction in multiscale systems. In C. P. Chang, M. Ghil, M. Latif, & J. M. Wallace (Eds.), *Climate change: Multidecadal and beyond* (pp. 67–80). Singapore: World Scientific Publishing Co./Imperial College Press.
- Zaliapin, I., Foufoula-Georgiou, E., & Ghil, M. (2010). Transport on river networks: A dynamic tree approach. *Journal of Geophysical Research*, *115*, F00A15. <https://doi.org/10.1029/2009JF001281>
- Zaliapin, I., Keilis-Borok, V., & Ghil, M. (2003a). A boolean delay equation model of colliding cascades. Part I: Multiple seismic regimes. *Journal of Statistical Physics*, *111*(3-4), 815–837. <https://doi.org/10.1023/A:1022850215752>
- Zaliapin, I., Keilis-Borok, V., & Ghil, M. (2003b). A Boolean delay equation model of colliding cascades. Part II: Prediction of critical transitions. *Journal of Statistical Physics*, *111*(3-4), 839–861. <https://doi.org/10.1023/A:1022802432590>